HAER
IOWA
85-AMES,
5-

STRUCTURAL STUDY OF REINFORCED CONCRETE ARCH BRIDGES
Iowa Department of Transportation
Ames
Story County
Iowa

HAER No. IA-89

WRITTEN HISTORICAL AND DESCRIPTIVE DATA

HISTORIC AMERICAN ENGINEERING RECORD
National Park Service
Washington, DC

HISTORIC AMERICAN ENGINEERING RECORD

STRUCTURAL STUDY OF REINFORCED CONCRETE ARCH BRIDGES

HAER No. IA-89

HAER
IOWA
85-AMES,
5-

Location:	Iowa Department of Transportation Ames, Story County, Iowa
Dates of Construction:	1894, 1910, 1917
Designer/Builder:	Various — See HAER documentation for individual structures
Present Use/Owner:	Various — See HAER documentation for individual structures
Engineer:	Dawn M. Harrison, August 1996
Project Information:	Three reinforced concrete arch bridges, built in the late nineteenth and early twentieth century by three prominent engineers promoting this type of bridge design, were selected for engineering analysis and evaluation based on modern structural theory and structural theory as it was known at the time the bridges were constructed. The project was part of the Iowa Historic Bridges Recording Project II, conducted during the summer of 1996 by the Historic American Engineering Record (HAER). Dr. Dario Gasparini, Professor of Civil Engineering, Case Western Reserve University, Cleveland, Ohio, with assistance of civil engineering students Eugene M. Farrelly and Dawn M. Harrison, completed this project under contract with HAER. See HAER No. IA-15 for documentation of the Melan Arch Bridge in Rock Rapids (1894).

INTRODUCTION

Reinforced concrete had its beginnings in the mid-nineteenth century with Jean-Louis Lambot's 1850 fabrication of a concrete boat.[1] However, Joseph Monier, a Parisian gardener, is generally credited with the invention of this widely-used composite material.[2] In 1861, he began manufacturing large flower pots using a pattern of reinforcement known as the "Monier Trellis."[3] His reinforcement system, patented in 1865, used wire nets embedded in concrete (Figure 1).[4] The invention was soon used for water and gas tanks, tubes and sewers, flat floors, and finally vaults and bridges. This new application was most widely accepted in Germany, where the use of concrete in bridges was common. In America, the first use of concrete in combination with iron arose in an effort to fireproof iron. In 1875, W. E. Ward constructed a building which included concrete walls, floor beams, and a roof reinforced with iron.[5] Ward's building, located in Port Chester, New York, was the first reinforced concrete structure built in the United States.[6]

Two pioneering concrete-iron bridge designers in the United States were Friedrich von Emperger and Edwin Thacher. In 1894, Emperger built the first American concrete-iron bridge using a system of reinforcement patented by an Austrian, Joseph Melan, in 1893. It was a 30'-0"-span, closed-spandrel arch in Lyon County, Iowa. Although Thacher states that "previous to this time no concrete-steel bridges of any importance had been built in the United States," Ernest L. Ransome did build the first reinforced concrete bridge in America.[7] The Alvord Lake Bridge, constructed in 1889, was designed to carry carriage traffic over a pedestrian pathway in San Francisco's Golden Gate Park.[8] However, the Lyon County bridge was the source of a national, long-term, influential concrete bridge design lineage, defined by the work of Emperger, Thacher, William Mueser and their Concrete-Steel Engineering Company. Competing reinforced concrete arch bridges were patented and built, almost contemporaneously, by Daniel B. Luten. Somewhat later, James B. Marsh patented and built his reinforced concrete "rainbow arches".

This report intends to add to understanding of the development of American reinforced concrete design by studying the structural design of three reinforced concrete arch bridges in Iowa:

- The Melan arch in Lyon County (1894)
- The Luten arch in West Union (1910)
- A Marsh arch in Boone County (1917)

The first two bridges are closed-spandrel arches, while the third bridge is an open-spandrel arch more characteristic of those built today. The three bridges' arch axes and reinforcement patterns are quite different. The bridges embody different design concepts, different understanding and application of arch theory, and represent different stages in the development of reinforced concrete technology. The nature of the differences is explored in this report through detailed geometric modeling, static structural analyses, and studies of static structural behavior. To provide a basis for understanding and evaluation, important concepts of arch theory and of reinforced concrete technology are discussed first.

ARCH THEORY

Arches are an ancient structural form and the development of their design methods has a rich history. Heyman and Addis give accounts of developments, principally for masonry arches.[9] The books of Joseph Melan (1908, translated to English by David Steinman in 1915), Malverd Howe (1897), and Joseph Balet (1907) are representative of the state of arch theory in the late nineteenth and early twentieth century when reinforced concrete began to be widely used.[10] These contemporary works define sophisticated (perhaps even daunting to engineers at the time) linear elastic models, more suitable to steel and reinforced concrete than to masonry. The books provide guidelines for design decisions regarding an arch's:

- Form (e.g. open- or closed-spandrel) and boundary conditions.
- Rise-to-span ratio.
- Centroidal axis shape.
- Cross-sectional area and moment of inertia at any position.

An important property of an arch form is its static determinacy. If a form is statically determinate, forces and bending moments at all points along the arch axis may be determined, regardless of material properties, using only force and moment equilibrium equations. This simplifies design considerably. Moreover, temperature changes and support settlements do not induce significant forces and moments in statically determinate forms. A classic statically determinate form, well-known prior to 1894, is the three-hinged arch. The arch has three hinges, or locations of zero bending moment: two at the supports and one at mid-span (Figure 2). Three-hinged arches were widely used for iron and steel structures, for example the 1889 Palais des Machines, whose arches span 350'-0" with a rise of 137'-0".[11] According to Emperger, the first reinforced concrete three-hinged arch was a Melan bridge at Steyer, Austria, built in 1898. The Steyer arch spanned 137.8' and rose only 8'-8".[12]

Static analysis of a three-hinged arch provides insight into parameters affecting an arch's thrust. Consider a three-hinged arch under a uniform distributed loading, q (Figure 3). By static equilibrium, the vertical reaction force, V, is equal to $qL/2$ and the horizontal thrust, H, is equal to $qL^2/(8h)$, where:

q = vertical distributed loading
L = span length
h = arch rise or height

Figure 4 is a free-body diagram of the same arch, cut at the middle hinge. It shows the reaction forces as well as the force required at the middle hinge to satisfy equilibrium. These forces show that the thrust at mid-span varies inversely with the rise, *h,* and directly with the square of the span, *L.* Also, the axial force in the arch increases from mid-span to support.

In a "fixed-fixed" arch, supports resist rotation as well as displacement (Figure 5). A fixed-fixed arch is the natural form for masonry, and was used for the earliest reinforced concrete arches. This form is statically indeterminate, meaning that forces and moments along the axis can be found either by an "exact" analysis accounting for elastic properties of concrete, or by approximate analyses.

Figure 6 shows a cross section through an arch with rib thickness, *a,* and width, *b.* Also shown are axial force, *N,* shear force, *V,* and bending moment, *M,* acting at that particular section. Stresses are calculated from these forces and parameters *a* and *b.*

The stress due to the axial force is simply the axial force, *N,* divided by cross-sectional area, *ab.* The stress due to the bending moment is the moment, *M,* divided by another geometric property called the section modulus. The section modulus for a rectangular beam is its moment of inertia divided by half its depth, equal to $ba^2/6$. Because masonry cannot resist bending moments well, a long-standing goal of designers of arches and domes was to determine an arch axis that minimizes bending moments for a dominant gravity loading condition. These axis shapes were called "equilibrium curves," "funicular curves," or "thrust lines". By the nineteenth century's end, several thrust lines corresponding to common load conditions were well-known (Table 1 and Figure 7).

Table 1. Thrust lines for common arch loading conditions.

Load Condition	**Corresponding Thrust Line**
Concentrated gravity forces	Piece-wise linear curve
Uniformly distributed load normal to axis	Circular arc
Gravity load uniformly distributed along horizontal projection	Parabola
Gravity load uniformly distributed along the axis	Catenary
Gravity load proportional to distance between the axis and a horizontal line above the axis	Transformed catenary

Figure 7e shows the transformed catenary, cited by both Luten and Howe as the thrust line for a gravity loading that varies with the distance between the arch axis and a horizontal line above it.[13] The general form of the equation is

$$y = r\left(\frac{m}{2}\right)\left(e^{x/m} + e^{-x/m}\right) \tag{1}$$

where y is the height of the arch axis at a horizontal coordinate x, and m is a geometric parameter. This equation differs from that of the common catenary by the ratio r. The transformed catenary was deemed appropriate for a filled-spandrel arch if the weight of the fill was dominant and its resultant pressure was downward.

With the exceptions of the circular arc and the piece-wise linear curve (Maillart's choice), all the other thrust lines have continuously varying radii of curvature, which significantly complicates the construction of the centering or falsework for the arch. Therefore, it was necessary to approximate such thrust lines with "many-centered" arches, that is, arches that consist of several circular arcs with different radii. The three-centered arch was commonly used (Figure 8).

Once the arch form, the rise-to-span ratio, and the shape of the arch axis are chosen, the arch's cross-sectional area and moment of inertia must be determined at all points. This requires estimating axial forces and moments at all sections, then sizing the section so stresses in concrete and steel are below allowable values. The simplest solution is to design a prismatic arch, i.e., an arch with a constant cross section along its span.

In addition to the above issues which have existed since the arch form's origin, the pioneers of reinforced concrete arch design faced new design issues unique to a composite material. How do concrete and steel work together to carry the axial force and bending moment at each section? How should the concrete and steel be sized? Where should the steel be placed?

CEMENT, CONCRETE, AND REINFORCEMENT TECHNOLOGY

Concrete consists of two main components, paste and aggregate. The paste is a cement-water mixture that binds the aggregates into a rocklike mass. The cement used today is known as Portland cement, and was invented by Joseph Aspdin, an English mason, in 1824.[14] Prior to Portland cement's invention, natural cements with a large raw material content were used in the United States. The advantages of Portland cement — greater strength, resistance to abrasion, and durability — led to its dominance. The first shipment of Portland cement arrived in the United States in 1868, and the first domestic Portland cement was produced at a plant in Coplay, Pennsylvania, in 1871.[15] As the reinforced concrete industry grew in America, so did the use of Portland cement. According to Thacher,

> Nothing can give a better idea of the growth and magnitude of concrete and concrete-steel construction in the United States during the past ten or twenty years than an inspection of . . . the diagram, [Figure 9], showing the quantity of cement consumed.[16]

Figure 9 shows several trends in American cement use from the year 1893 to the year 1902. Prior to 1897, more foreign (primarily German) Portland cement was used than American cement. Beginning in 1896, just two years after the Melan reinforced concrete bridge was introduced in the United States, there are dramatic yearly increases in consumption. In 1902, approximately 90 percent of the Portland cement consumed in the United States was American-made. The graph also shows the decline in popularity of American natural cements.

In addition to the type of cement, another important parameter affecting concrete's strength is the water-cement ratio. Although specific information regarding the effects of water-cement ratio was not available when he wrote, Thacher does state that through the year 1904, the majority of American engineers used a "dry" concrete mixture.[17] He states that soon thereafter, "wet" mixtures became more common. Since the terms "wet" and "dry" do not allude to exact ratios, no conclusions can be drawn. It is useful to note that in general, concrete with a relatively small water-cement ratio (0.4) may have a compressive strength almost 50 percent greater than concrete with a larger water-cement ratio (0.7).[18] However, dryer mixtures are less workable and require more tamping to achieve consolidation.

The second component of concrete is aggregate, usually consisting of sand, gravel, and crushed stone. During the late nineteenth and early twentieth centuries, it was common practice to proportion concrete mixes by weight. Several Melan bridges, including those at the Vanderbilt estate in New York and the arch at Stockbridge, Massachusetts used a 1:2:4 ratio of Portland cement to sand to broken stone.[19] Aggregate is generally graded, consisting of a variety of sizes, to minimize the cement needed to bind the material. It was not until the early twentieth century, however, that Americans used graded aggregate. In 1905 John Sewell states that many engineers previously regarded aggregate of uniform size necessary to obtain favorable results. He writes:

> It has always been realized that an ideal concrete was one in which all the interstices of the sand, or finder parts of the aggregate were filled with cement, and all the larger voids were filled with the mortar thus formed. Until recently, many American engineers considered that stone or gravel of uniform size was quite necessary to the best results; for a number of years, however, many officers of the Corps of Engineers have used a graded aggregate, thus securing a better result with less cement. The writer believes that this is now generally regarded as the best practice.[20]

At the turn of the century, the strength properties of concrete were still under experimental investigation. Sewell cites 2,000 to 3,000 pounds per square inch (psi) as the compressive strength of a moderate concrete in 1902, admitting 2,000 psi to be on the conservative side.[21] Presently, a value of 3,000 to 5,000 psi is accepted as the compressive strength of most concretes, and the tensile strength ranges from 274 to 530 psi. In 1894 Emperger cites 250 psi as an accepted value of concrete's tensile strength and 1.5×10^6 psi as its modulus of elasticity.[22] Emperger's elastic modulus is approximately half the value of the 3.0×10^6 psi commonly used today. The use of a very conservative value for the elastic modulus was characteristic of the relatively new concrete-steel industry.

Nearly all early designers accepted a value of 30×10^6 psi for the elastic modulus of steel, approximately ten times that of concrete. According to F. E. Turneaure and E. R. Maurer, there were three different grades of reinforcing steel: soft, medium, and hard, each with a different tensile strength (Table 2).[23]

Table 2. Ultimate tensile strength for various grades of reinforcing steel. From Turneaure and Maurer, *Principles of Reinforced Concrete Construction* (New York: Wiley, 1908).

Grade of Reinforcing Steel	Ultimate Tensile Strength (psi)
Soft	50,000 - 60,000
Medium	60,000 - 70,000
Hard	80,000 - 100,000

In addition to the strength properties of steel, pioneering reinforced concrete designers had to select the type of reinforcement bar: cold rolled sections such as I- or T-bars, round bars, or flat plates. An illustration from Robert E. Loov's "Reinforced Concrete at the Turn of the Century" shows some of the patented reinforcing bars in use at the turn of the twentieth century (Figure 10). One of the most widely-used early reinforcement bars was the Ransome bar, patented by Ernest Ransome in 1889. In *Principles of Reinforced Concrete Construction* (1908), Turneaure and Maurer state that flat bars did not adhere to concrete as well as round or square designs.[24] The presence of corrugations, crimps, and protrusions on these bars was an attempt by early designers to increase the mechanical bond between concrete and steel, as can be seen in the Hyatt, Thacher, and DeMan bars. In addition to round, square, or flat bars, rolled sections (I- or T-bars and angles) were also used. Melan pioneered the use of rolled sections in reinforced concrete construction with the introduction of his system in 1893.

In a reinforced concrete arch, the steel can be placed along the intrados, extrados, or center of the rib. Since concrete's tensile strength is much less than its compressive strength, steel should be placed at locations where the concrete may experience tensile stresses. Figures

11 and 12 show six different cross sections through a reinforced concrete arch. The behavior of any reinforced concrete section depends on:

- The eccentricity, *e*, of the steel's centroid with respect to the concrete's centroid.
- The bond (or interlocking) between steel and concrete.
- The steel's moment of inertia, I_S, with respect to its own centroid.
- Whether the concrete is cracked or uncracked.

A brief explanation of the important arrangements used in early reinforced concrete arches follows. Uncracked concrete is assumed throughout.

For reinforcement placed with zero eccentricity, so that the centroidal axes of concrete and steel coincide, behavior is unaffected by material bond. It is irrelevant whether concrete and steel are bonded (acting as one composite material) or unbonded (acting as two separate beams in parallel). At any cross section there is a resultant axial force, *N*, and a resultant moment, *M*. The steel and the concrete share the resultants in the following proportions:

$$\frac{N_S}{N_C} \propto \frac{E_S A_S}{E_C A_C} \tag{2}$$

$$\frac{M_S}{M_C} \propto \frac{E_S I_S}{E_C I_C} \tag{3}$$

where:

N_S = Axial force in steel
M_S = Bending moment in steel
N_C = Axial force in concrete
M_C = Bending moment in concrete
A_S = Cross-sectional area of steel
I_S = Moment of inertia of steel
A_C = Cross-sectional area of concrete
I_C = Moment of inertia of concrete
$N = N_S + N_C$
$M = M_S + M_C$

Note that reinforcement of the type shown in Figure 11b carries practically no moment because I_S is insignificant.

If the reinforcement in Figure 11 were placed with a nonzero eccentricity, *e*, structural behavior strongly depends on whether there is an effective bond between concrete and steel. If there is no bond, the behavior will be the same as for the case of zero eccentricity. If there is a perfect bond, the reinforced concrete will truly act as a composite material, with a transformed centroid and a transformed moment of inertia.

In Thacher-type reinforcement, steel is placed symmetrically in the section, so the eccentricity is zero (Figure 12). The behavior again strongly depends on whether there is an effective bond between the concrete and steel. Because the steel at the top and bottom is not connected, if there is no concrete-steel bond, the steel will not carry any significant bending moment because I_S is small.

The principal conceptual issue on the design of reinforcement is whether or not to assume perfect adhesion (or interlocking) between the concrete and the steel. If perfect adhesion is assumed, i.e., true composite behavior occurs, then a steel web connecting reinforcement along the two faces of an arch is not necessary for resisting moments (though it helps to carry shear forces). Additionally, there are practical issues of ease of fabrication (bending and splicing reinforcement) and placement and compaction of concrete around reinforcement.

DESIGN AND CONSTRUCTION OF REINFORCED CONCRETE ARCH BRIDGES

Extensive information on the development of reinforced concrete arch bridges is provided by two papers by Emperger in the American Society of Civil Engineers (ASCE) *Transactions,* one in 1894 and another ten years later.[25] Turn-of-the-century texts on reinforced concrete by Reid, Buel and Hill, Turneaure and Maurer, Taylor and Thompson, Howe, Considere, Morsch, Colby and others (see Kemp) provide further insight.[26] These works discuss various arch forms — rigid-frame, closed-spandrel, open-spandrel, tied, three-hinged — and a variety of reinforcing systems.

Emperger begins by discussing European Monier arches built in the 1880s, reinforced with a net of iron rods. He notes that such nets have no stiffness prior to the hardening of the concrete and that "this difficulty has been overcome by the other systems now in use, which use rolled shapes instead of wire netting." As a first example, Emperger describes the system invented in 1884 by Robert Wünsch of Budapest, Hungary. The system is essentially a rigid frame with a haunched girder (Figure 13). Buel and Hill describe two European bridges of the Wünsch type.[27] Ernest Ransome's 1889 Alvord Lake bridge may be of a Wünsch form.

As a second example, Emperger discusses the Melan system, patented in Austria in 1892 and in the United States in 1893.[28] Melan's patent is the source of an important lineage of reinforced concrete bridge design in the United States. That lineage is perhaps best illustrated by an advertisement for the Concrete-Steel Engineering Company appended to Reid's 1907 text

(Figure 14). The advertisement implies a continuity in the designs of Melan, Emperger, Thacher, and Mueser. Illustrations show a Melan arch built on the Vanderbilt estate at Hyde Park, New York, in 1898; a Thacher reinforcing bar; and the modern reinforcing bar patented by Mueser.

Melan's 1893 patent is for a prismatic arch with a cross section of rammed concrete between steel I-beams (Figure 15). The concrete and steel act in parallel and have the same deflections. The structural behavior does not depend on the adhesion between concrete and steel, therefore they do not truly form a new, composite material.

Emperger, in his 1897 patent, states that "the use of metal in the core of a vault or arch is useless. . . ."[29] Moreover, he notes that the smallest rolled I-beams are too large for small spans and that accurate bending for large radii of curvature is difficult. He thus patents a new reinforcing system (Figure 16).

Emperger's system consists of a pair of steel sections, one near the inner surface (intrados) and the other near the outer surface (extrados) connected either by "distance rods" or by a lattice. The behavior of the section with latticed reinforcement does not depend on adhesion between steel and concrete, whereas adhesion controls the behavior of reinforcement with "distance rods".

Neither Melan's centered I-beam reinforcement nor Emperger's centered latticed reinforcement relies on the adhesion or the interlocking between concrete and steel to assure equal strains and thus true composite behavior. Thacher recognized that if the concrete and steel can be made to have the same strains, then latticing is not needed. He patented a series of reinforcing bars that improved the mechanical interlocking between the steel and the concrete. Figure 17 shows the reinforcing system and the bars patented by Thacher in 1899.[30]

Thacher claimed to provide an

> effective connection between the bars and the concrete, employing lugs, dowels, bolts or rivets, which pass through the bars and project into the concrete, in which they are embedded, and thereby reinforce the adhesion between the metal and the concrete

and that the bars were "readily and cheaply spliced," "readily bent," and could be "stored or shipped in straight form". He understood that "the bars act as the flanges of beams to resist bending moments, whereas the shear stresses, which are small, are taken by the concrete alone". He noted that the absence of latticing

> enables me to completely embed the lowermost member of the pair before the uppermost is placed, thereby securing intimate contact between the bar and

concrete without requiring the great particularity of filling and ramming that is necessary where a bent I-beam with extending flanges is employed.[31]

Thacher continued to improve reinforcing bars, patenting additional forms in 1902 (Figure 18) and then the "Thacher patent bars" shown in Reid's 1907 text (Figure 14).

Luten, an important competitor to the Concrete-Steel Engineering Company, is the subject of a forthcoming biography.[32] Luten graduated from the University of Michigan in 1894, taught at Purdue University in Indiana, and then entered private consulting practice in 1900, aggressively promoting reinforced concrete arches and protecting his designs with patents.[33] Luten's 1900 article in the *Railroad Gazette* shows the form that was the focus of Luten's design practice: the closed-spandrel tied arch (Figure 19).

Figure 19 shows a model of an unreinforced arch, tied with two timbers for resisting the horizontal thrust. His tied arch design evolved further in 1902 (Figure 20). Its principal features are:

- A curved reinforced concrete tie, below the streambed, with flanges to prevent scour.
- Reinforcement consisting of plain round bars, bent to the arch face that may be in tension.
- An arch axis that is a three- or five-centered approximation to the transformed catenary.

Luten preached that the concrete tie decreased the size of footings and "flood-proofed" his bridges, i.e., scour around the abutments would not collapse the arch. Luten understood that the directions of the earth pressures caused by the fill were uncertain, but he believed that the transformed catenary, or an approximation of it, was an "optimum" shape for a filled-spandrel arch.[34]

Other designers developed independent reinforced concrete arch systems at the same time as Luten. For example, a 1994 article by Snyder and Mikesell discusses turn-of-the-century reinforced concrete arches built in California. The article focuses on accomplishments of engineers John G. McMillan, John Leonard, and William Thomas, who designed primarily closed-spandrel forms (the reinforcing systems are not described).[35] Thomas' "Thomas System" bridges were three-hinged, open-spandrel precast concrete arches. "More than a dozen" such forms were built by 1914.[36] The 1908 Water Street Bridge in Santa Cruz, California, remains in use though in a modified form.[37]

On August 6, 1912, James B. Marsh of Des Moines, Iowa, patented the open-spandrel reinforced concrete arch (Figures 21 and 22).[38] His design became known as the "rainbow arch". HAER Nos. IA-29 and IA-46 discuss Marsh and his bridges in Iowa.

The open-spandrel arch form is more adaptable to a variety of topographic conditions because the deck may be placed at any elevation on the arch axis (Figure 23). An open-spandrel arch is more practical for longer spans than the closed-spandrel form because it does not need to carry the weight of fill and spandrel walls. Drainage of water from the deck is more easily accomplished in open-spandrel arches. The closed-spandrel form soon fell into disuse. The ASCE Special Committee in Concrete and Reinforced Concrete Arches, authorized in 1923, published its final report in 1935. This report states, "No work has been done on spandrel-filled arches. . . ."[39]

The distribution of dead load in an open-spandrel arch differs from that of a closed-spandrel arch. The horizontal deck is generally the dominant gravity load of an open-spandrel arch. Therefore a parabolic arch axis becomes more suitable for minimizing bending moments (Figure 7). An important issue in modeling of open-spandrel arch is the continuity and interaction between the arch, the vertical elements, and the deck. The deck may be designed to serve several purposes: to transfer local vehicle loads to the vertical elements, serve as a tie to resist thrust, or provide sufficient flexural stiffness so the arch carries principally axial forces (Maillart's choice). But these design issues appeared later, long after Emperger carried out his pioneering design in Rock Rapids, Iowa, in 1894.

AUSTRIAN CONCRETE-STEEL ARCHES AND EMPERGER'S 1894 PAPER

Emperger's 1894 paper discusses the analysis of the 13'-0" Melan arch bridge (Figure 24), tested by the Austrian Society of Engineers and Architects.[40] Figure 24 shows that the Austrian arch was not truly reinforced concrete, but rather concrete used in parallel with steel (Figure 25). The arch's behavior is independent of the bond between concrete and steel. Nonetheless, a structural analysis is performed on this structure to evaluate the accuracy of Emperger's formulas, which may have been used to design the Rock Rapids bridge in 1894.

The first step in analyzing of the Melan arch is to calculate cross-sectional areas and moments of inertia for both steel and concrete, noting the moduli of elasticity, additional section properties, and working load conditions given by Emperger in his 1894 paper. The weight and cross-sectional area noted by Emperger are used to estimate the moment of inertia.

Table 3. Steel and concrete properties for 13'-0" Melan arch model.

Property	Steel	Concrete
width (ft)	—	3.1
depth (in)	3.125	3.125
weight (lb/ft)	4.3	140
modulus of elasticity (psi)	$E_S = 30 \times 10^6$	$E_C = 750{,}000$
cross-sectional area (in^2)	$A_S = 1.264$	$A_C = 124.93$
moment of inertia (in^4)	$I_S = 2.378$	$I_C = 100.28$
section modulus (in^3)	$R_S = 1.522$	$R_C = 64.69$

Emperger considers a vertical distributed load of 718 lb/ft extending over half of the span, which is divided into a dead load of 144.72 lb/ft and a live load of 573.28 lb/ft.

The arch is modeled as a plane frame composed of straight beam-column segments. Each segment consists of a steel and a concrete element in parallel. Theoretically, the more segments used, the more accurate the analysis, so 5-, 6-, and 10-segment models are analyzed to observe the convergence of the results (Figure 26). A parabola is chosen as the shape of the arch axis. Several important quantities reveal similarities in the results of the three analyses (Table 4).

Table 4. Variation of results with number of segments in 13'-0" Melan arch model.

Number of Segments	Horizontal Thrust (kips)	Moment at Abutment (kip-ft)	Moment at Crown (kip-ft)
5	9.903	-1.8830	—
6	9.922	-1.8444	0.2972
10	9.972	-1.9410	0.2957

Table 4 shows small variations in the values presented with the number of segments used. The remainder of this discussion will refer to the results of the 10-segment analysis only.

Emperger gives a set of formulas that form the basis of the Austrian design, which shall be briefly evaluated. Letting the total load, Q, be equal to the sum of that carried by the concrete, Q_C, and the steel, Q_S, Emperger states:

$$Q = Q_C + Q_S \tag{4}$$

$$\frac{Q_C}{Q_S} = \frac{E_C I_C}{E_S I_S} = \gamma \tag{5}$$

Emperger's equation (Eq. 5) is not exactly correct because only the ratio of the moments, not the ratio of "loads," depends upon the ratio of moments of inertia.

Emperger then states that the concrete and steel stresses S_C and S_S are:

$$S_C = \left(\frac{N}{d} \pm \frac{6M}{d^2}\right)\left(\frac{\gamma}{1 + \gamma}\right) \tag{6}$$

$$S_S = \left(\frac{N}{A_S} \pm \frac{M}{R_S}\right)\left(\frac{a}{1 + \gamma}\right) \tag{7}$$

Equations 6 and 7 are also not correct because in an arch the total axial force is shared in proportion to $E_C A_C / E_S A_S$ and the total moment is shared in proportion in $E_C I_C / E_S I_S$.

Table 5 lists maximum stresses for each of the ten arch segments (numbered as in Figure 26), determined from a modern analysis of a half-loaded span. The second column lists the stresses at the extrados, while the third column lists the stresses at the intrados.

Table 5. Concrete stresses in 13'-0" Melan arch for half-span loading (negative numbers indicate compression).

Segment	Stress at Extrados (ksi)	Stress at Intrados (ksi)
A	0.1315	-0.2381
B	-0.0103	-0.0935
C	0.0021	-0.1040
D	0.0446	-0.1453
E	0.0375	-0.1378
F	-0.0221	-0.0784
G	-0.0121	-0.0889
H	0.0169	-0.1182
I	0.0052	-0.1066
J	-0.0438	-0.0577
K	-0.1337	0.0322

Table 6. Steel stresses in 13'-0" Melan arch for half-span loading (negative numbers indicate compression).

Segment	Stress at Extrados (ksi)	Stress at Intrados (ksi)
A	5.2754	-9.5408
B	-0.4107	-3.7449
C	0.0892	-4.1663
D	1.7903	-5.8199
E	1.5069	-5.5211
F	-0.8855	-3.1408
G	-0.4797	-3.5602
H	0.6822	-4.7331
I	0.2115	-4.2700
J	-1.7536	-2.3094
K	1.2924	-5.3553

These stresses are well within allowable values for each material. Emperger states that for a half-loaded span, the horizontal thrust, H, is:

$$H = \frac{1}{8}\left(q + \frac{p}{2}\right)\left(\frac{L^2}{r}\right) \qquad \textbf{(8)}$$

where:

q = dead load
p = live load
L = span
r = rise

Figure 27 shows a three-hinged arch with a distributed dead load across the entire span and a live load across half of the span. H_L and H_R are the horizontal thrusts for the left and right halves of the arch, while V_L and V_R represent the vertical reactions. By static equilibrium:

$$V_L = \frac{1}{2}\left(q + \frac{3p}{4}\right) \qquad \textbf{(9)}$$

$$H_L = \frac{1}{8}\left(\frac{L^2}{r}\right)\left(q + \frac{p}{2}\right) \qquad \textbf{(10)}$$

This completely agrees with Emperger's equation for the horizontal thrust of a half-loaded span (Eq. 8).

For a fully-loaded span, Emperger states

$$H = \frac{1}{8}(q + p)\left(\frac{L^2}{r}\right) \qquad \textbf{(11)}$$

Figure 28 represents a three-hinged arch with both dead and live load distributed across the full span. Again, by static equilibrium:

$$V_L = \frac{1}{2}(q + p) \qquad \textbf{(12)}$$

$$H_L = \frac{1}{8}\left(\frac{L^2}{r}\right)(q + p) \tag{13}$$

These results agree with Emperger's equation (Eq. 11). It is clear that Emperger used the statically determinate three-hinged arch model to approximate the horizontal thrusts at the supports of Melan's statically indeterminate fixed-fixed design. To evaluate the accuracy of these formulas, ten different models are analyzed (Table 7).

Table 7. Models used to test Emperger's three-hinged arch approximation.

Model	Load Case	Span, *L*, ft	Rise, *r*, in
I	live load on half span	13.33	11.0
II	live load on full span	13.33	11.0
III	live load on half span	13.33	16.5
IV	live load on full span	13.33	16.5
V	live load on half span	13.33	22.0
VI	live load on full span	13.33	22.0
VII	live load on half span	19.69	11.0
VIII	live load on full span	19.69	11.0
IX	live load on half span	26.25	11.0
X	live load on full span	26.25	11.0

Table 8 lists the horizontal thrusts calculated using Emperger's sixth and seventh equations (Eq. 8 and 11) as well as those resulting from the modern analysis.

Table 8. Comparison of modern structural analysis to Emperger's formulas for horizontal thrust.

Model	Horizontal Thrust (kips)	Horizontal Thrust (kips) Emperger
I	9.075	9.027
II	14.741	15.024
III	6.525	6.262
IV	10.358	10.423
V	5.118	4.764
VI	7.909	7.930
VII	19.464	19.675
VIII	32.013	32.747
IX	34.460	34.978
X	56.960	58.218

The similarity of these results show that the three-hinged arch model is very effective for approximating horizontal thrusts in a fixed-fixed arch.

Emperger also gives formulas for the moment in the crown and the moment in the abutment for a fully-loaded fixed-fixed arch. Values computed using Emperger's formulas are compared to results from modern analyses (Table 9).

Table 9. Comparison of modern structural analysis to Emperger's formulas for bending moments.

Model	Moment in Crown (kip-ft)	Moment in Crown (kip-ft) Emperger	Moment in Abutment (kip-ft)	Moment in Abutment (kip-ft) Emperger
II	0.493	0.347	-0.889	-0.695
IV	0.220	0.161	-0.415	-0.321
VI	0.129	0.091	-0.238	-0.183
VIII	1.111	0.757	-1.971	-1.513
X	1.844	1.345	-3.479	-2.691

Emperger also lists four material characteristics of concrete and steel which, in his opinion, make them "especially fit to be used together." These are as follows:

- The large difference in elastic moduli of concrete and steel allows concrete to carry a small load while steel simultaneously carries a larger load.
- If the cohesion between concrete and steel is larger than the tensile strength of concrete, then the bond "acts like a glue" when hardened.
- "Concrete is the best conservator of iron."[41]
- The similar coefficients of thermal expansion for concrete and steel preclude the occurrence of secondary stresses due to temperature changes.

These statements did not go unnoticed by American engineers. In the discussion following the Emperger article, several issues were addressed. One major concern was for the effect of thermal expansion on material bond. Many could not believe that the thermal expansion of concrete and steel could be similar. One writer states, "The remarkable fact . . . that the thermic expansion of Portland cement is within 2/10,000,000 parts the same for both materials for 1 degree Celsius may, for want of sufficient data, go unchallenged, but surely, steel being a better conductor of heat than concrete, there must be considerable difference, at the same moment, in the expansion of the two materials."[42] Another writer comments:

> Another and even more serious source of danger to that bond would be the effect of changes of temperature. . . . Under changes of temperature the iron will be heated or cooled much quicker, and to a far greater extent, with a corresponding greater expansion or contraction, than the neighboring concrete. . . . That the result would be disastrous to the bond seems clear.[43]

This writer also states, "It would . . . seem advisable to introduce iron rods between the ribs, to prevent them from spreading, and not to trust to the rather uncertain adhesion between the two materials."[44]

Currently, concrete's coefficient of thermal expansion is known to be approximately 6×10^{-6} per degree Fahrenheit while steel's is 6.5×10^{-6} per degree Fahrenheit.[45] These values are obviously similar and Emperger's assumptions on this matter are indeed correct.

In addition, several comments specific to the Melan system were made to Emperger. One comment by W. R. Hutton shows understanding of steel's role:

> In [the Melan system], no attempt is made to supply directly with metal the deficiency in tensile strength of concrete. It is a combination in one structure of materials entirely distinct in their characteristics, in which combination the

> moment of inertia of the sections is inversely proportioned to the modulus of elasticity of each material.[46]

Hutton's statement is correct. The 13'-0" Melan arch tested by the Austrian Society of Engineers and Architects was a prismatic arch, with the steel placed at the center of the concrete. There was no attempt made to place the steel where tensile stresses would occur, nor to take advantage of adhesion to achieve true composite behavior.

MELAN-EMPERGER ARCH AT ROCK RAPIDS, IOWA

The Rock Rapids bridge was one of eighteen built by contractor William S. Hewitt in Lyon County in 1894. Rock Rapids was a small city, less than a decade old, and neither steel I-beams nor "fine quality" cement was readily available, all of which made this location an unlikely choice for an innovative reinforced concrete bridge. Historian Juliet Landler writes:

> Yet, what Lyon County lacked in material goods, it made up for in pioneer spirit, and perhaps this is what first attracted Hewitt. The early settlers shared a love for the new and the unexplored and many were looking to make their mark on the world.[47]

Whatever the reason, this small city in northwest Iowa is the site of the first reinforced concrete bridge in the United States using the Melan system. Construction began in June using German cement that cost $3.00 per barrel.[48] The concrete mixture, characteristic of many early Melan bridges in the United States, was a 1:2:4 ratio of cement to sand to broken jasper.[49] John Olsen was the builder chosen for the project. His choice to face the spandrel walls with Sioux Falls jasper was purely aesthetic. The bridge carried farm machinery and did not need much maintenance for the first 70 years. It was transported to a new location four miles away from the original site in 1964 when state highway officials declared its 16'-0" width too narrow.[50]

The first step in modeling the Rock Rapids Melan arch is to fit curves, using measurements from the initial site visit, to both the intrados and extrados of the arch ring. An ellipse is chosen as the thrust line and the equations are as follows:

$$\left(\frac{x - 5.3086}{5.3086}\right)^2 + \left(\frac{y}{2.073}\right)^2 = 1 \qquad \textbf{(14)}\ \text{Extrados}$$

$$\left(\frac{x - 5.3086}{4.572}\right)^2 + \left(\frac{y}{1.861}\right)^2 = 1 \qquad \textbf{(15)}\ \text{Intrados}$$

The location of the steel is the next issue to be addressed. A 3" flange width and a 1.5" concrete cover were measured at the site. For this model, concrete cover was kept constant for the span's entire length, by choosing an elliptical steel curve. With this information, the transformed section's centroid is calculated and plotted (Figure 29). The transformed centroid lies just slightly below the geometric center.

The area between the intrados and extrados is used to calculate the total amount of concrete. A density, γ, of 150 pounds per cubic foot (pcf) is used to calculate its weight. Similar calculations are used to calculate the dead weight contributions from the stone ($\gamma = 164$ pcf), earth fill ($\gamma = 100$ pcf), and steel (4.3 lb/ft). The results for the entire arch are shown below (Table 10).

Table 10. Total weights of various materials in the Rock Rapids bridge.

Material	Weight (kips)
Concrete	101.33
Steel	0.832
Earth fill	73.88
Masonry	9.195
Total	185.24

Finally, the arch is modeled using 58 straight, prismatic, fully composite beam-column segments. Whereas the model used to analyze the arch mentioned in Emperger's 1894 paper consists of unbonded beam-column elements in parallel, this model consists of single beam-column elements with transformed section properties using concrete's modulus of elasticity. This model assumes that the eccentrically-placed steel is perfectly bonded to the concrete. Perfect bonding is essential for achieving truly composite reinforced concrete behavior, an assumption implicit in modern reinforced concrete design. Transformed moments of inertia and cross-sectional areas are then calculated for each of the 58 beam-column elements. Detailed information regarding geometric modeling, formulas used, and exact results are listed in Appendix A.

The Melan Rock Rapids Arch is modeled as a plane frame having a total of 58 members and 59 nodes (Figure 30). Linear elastic analysis of a typical barrel width of 3.1' gives deflection, moment, and axial force results, from which stresses are calculated (Appendix A). Two cases are examined, one to observe the arch's behavior under its own dead weight, and a second case to evaluate its behavior under a live load of 100 pounds per square foot (psf) on one half of its span.

Under the arch's own weight, the axial forces are highest near the abutments, totaling about 17 kips, and decrease uniformly to approximately 13 kips at the crown. Figure 30 shows that the tangent of the curve varies between a vertical position at the abutments and a horizontal position at the crown. Therefore, the decrease in the magnitude of the axial force from the abutment to the crown is expected. The half-span live load adds only 2.5 kips to the maximum axial force.

The variation of cross-sectional area and moment of inertia with position governs which portion of the arch carries the greatest bending moments. Portions of the arch with the greatest cross-sectional area and moment of inertia will carry the largest bending moment. The results of the linear elastic analysis show that this is exactly the case. The bending moments are maximum at the supports, where cross-sectional area and moment of inertia are greatest, and minimum at the crown.

The stresses in concrete due to axial forces are maximum at the crown, where the effective cross-sectional area is smallest, and minimum at the abutments, where the effective area is largest. Stresses due to combined axial forces and bending moments range from +10.73 psi to -62.26 psi (negative indicates compression). These values are well within the allowable range for concrete and cracking is unlikely. Stresses in steel range from approximately +45 psi to -445 psi. These values are extremely small. Most structural steels yield at a stress of 30,000 psi or greater. The stresses indicate that the steel's cross-sectional area could have been substantially reduced. In addition, steel has the greatest tensile stresses under the live load condition near the abutment, reaching a maximum value of +305.96 psi. Considering that steel is added mainly to increase tensile strength, the arch's entire span does not need reinforcing steel.

The Rock Rapids arch is the source of the Concrete-Steel Engineering Company's reinforced concrete bridge design lineage. Now more than one hundred years old, it stands, with very little modification, the first of a substantial line of American reinforced concrete bridges built from the pattern of "System Melan."

REINFORCED CONCRETE ARCHES OF THE CONCRETE-STEEL ENGINEERING COMPANY

Concrete bridge building became a rage in the United States at the turn of the century and the Concrete-Steel Engineering Company was a leading design firm. Thacher, writing in 1904, states:

> Since that date (1894), the Concrete-Steel Engineering Company of New York City and their predecessors have built, or are now building, under the Melan, Thacher and von Emperger patents, about three hundred spans of concrete-steel bridges, distributed over nearly all parts of the United States.[51]

The role of the company in the design of one bridge, Dayton's Washington Street Bridge, is described by Simmons.[52] Concrete-Steel Engineering Company reinforcement systems were used by other designers. Table 11 gives a sample of completed bridges that used reinforcement systems developed by Melan, Emperger and Thacher.

The Eden Park bridge was begun almost immediately after the bridge at Rock Rapids. The Southern Boulevard Bridge in Detroit is an early example of a reinforced concrete railroad bridge and an early example of latticed-girder reinforcement. The 1902 Zanesville, Ohio, Y-Bridge includes Thacher bars without lacing. However, the later Dayton bridges reverted to a latticed-girder reinforcement.

Table 11. Bridges that utilize Melan, Emperger, or Thacher reinforcing systems.

Arch	Date	Span (ft)	Rise (ft)	Crown Thickness (in)	Reinforcement
(a) Eden Park, Cincinnati, OH	1894-1895	70	10	15	9", 21 lb I-beams, 36" o.c.
(b) Near Frederickstown, Knox County, OH	1896	50	5		52 lb rails, 24" o.c.
(c) Washington Street Bridge, Dayton, OH	1905-1906	7 spans, totaling 620	11.5 for the center 90' span	20 for the center 90' span	lattice girders, 36" o.c.
(d) Main Street Bridge, Dayton, OH	1902	7 spans: 2 @ 69, 2 @ 76, 2 @ 83, 1 @ 88	5.3-8.8	16-20	lattice girders, 36" o.c.
(e) Third Street Bridge, Dayton, OH	1905-1906	7 spans, totaling 710	9.67 for the center 110' span	19-25	lattice girders, 34" apart
(f) Hyde Park, NY (2 bridges)	1897-1898	Two spans: 1 @ 53, 1 @ 26 75	7.5 14.67	10 15	7" I-bms 5" I-bms 9" I-bms
(g) Southern Boulevard, Detroit, MI	1895-1896	48	9.5	18	15" deep lattice girders, 30" o.c.
(h) Stockbridge, MA, Pedestrian Bridge	1895	100	10	9	7", 15 lb I-beams, 28" o.c.
(i) Topeka, KS	1896-1898	5 spans: 2 @ 97.5, 2 @ 110, 1 @ 125	12	22	18" latticed steel girders, 36" o.c.
(j) Y-Bridge, Zanesville, OH	1902	81 - 122	various	various	Thacher bars w/o laced web

(a) "Concrete Arch Supplement," *Ohio Historic Bridge Inventory, Evoluotion, ond Preservotion Plon* (1994), p. 34.
(b) Ibid., p. 37.
(c) "Building the Washington Street Bridge in Dayton, Ohio," *Engineering Record*, vol. 55, no. 9 (March 2, 1907): 248-250.
(d) G. R. Stattelman, "Concrete Steel Bridges, Dayton, Ohio," *Report of the Twenty-Seventh Annual Meeting of the Ohio Engineering Society* (1906).
(e) "The Third Street Reinforced Concrete Bridge, Dayton, Ohio," *Engineering Record*, vol. 53, no. 12 (March 24, 1906).
(f) "Two Recent Melan Arch Bridges," *Engineering News*, vol. 40, no. 19 (November 10, 1898).
(g) "A Melan Concrete Steel Railroad Bridge," *Roilrood Gazette*, vol. 31 (March 3, 1899): 150-51.
(h) Friedrich von Emperger, "Melan Arch of 100' Span, Stockbridge, Massachusetts," *Engineering News*, November 7, 1895.
(i) R. W. Steiger, "Nineteenth-Century Kansas Comes of Age," *Concrete Construction*, March 1994: 271-274.
(j) David Simmons, "Building a Concrete Y," *Concrete Internotionol*, June 1992: 42-47.

LUTEN ARCH IN WEST UNION, IOWA

As stated before, Luten's arches had several features which differed from those of the Concrete-Steel Engineering Company. These included:

- Smaller, often undeformed, reinforcing rods (3/4" to 1" in diameter).
- Reinforcement placed along both intrados and extrados of the arch rib.
- A concrete tie to resist the arch's thrust.

To examine the effects of these features, three different analyses are performed. The first analysis models the Luten arch without the concrete tie, as a fixed-fixed arch. The second analysis includes a rectangular tie with 1" diameter tension rods placed 12" apart transversely across the width of the arch (Figure 31). The third model uses a concrete tie with a lip to prevent scour (Figure 20), which increases its cross-sectional area and moment of inertia.

Figure 32 shows a model of the reinforced concrete arch designed by Luten and constructed in West Union, Iowa, in 1910. In deciding upon a model for analysis, several assumptions are made. These include the arch axis shape, the intrados and extrados curves, the arch's size near its supports, the steel's location, and the concrete tie's size and shape. In Luten's 1902 article, "The Proper Curvature for a Filled Arch," he discusses the use of segmental arches for many of his filled-arch designs.[53] For this reason, the data points taken during the initial site visit are plotted and a three-centered arch is fit through these points for the curve of the intrados.

Figure 33 shows the three centers, located at approximately 20'-0", 44'-0", and 71'-0" below the springing of the arch. The corresponding radii are 40'-0", 70'-0", and 80'-0". The extrados of the West Union arch could not be measured and there are no drawings available showing the arch thickness. Therefore, to approximate the extrados curve, measurements are scaled from a drawing of an 80'-0" Luten arch located near Decatur, Indiana. This results in a crown measurement of 16" and a rib thickness of 6'-0" near the supports. Using these three points, a two-centered arch is fit for the curve of the extrados, with centers located at 60'-0" and 70'-0" below the springing of the arch. The respective radii are 70'-0" and 80'-0".

To determine the size of the concrete tie, information is taken from Luten's 1902 articles, "Design of a Concrete Steel Arch Bridge" and "Concrete Steel Bridges". The tie is assumed to be 8" thick, with a depression at its center of 6". The tie is plotted as a circular arc with a radius of approximately 900'-0". It is almost horizontal and spans the entire length of the bridge. For the second model, the steel is placed at the concrete tie's center, embedded 3.5". The gross section has an area of 8 ft^2 and a moment of inertia of 0.297 ft^4. The scour-preventing lip on the third model is assumed to be 3'-6" long, extending out at an angle of 45 degrees from horizontal (Figure 32). The concrete tie of the third model has an area of 13.32 ft^2, and a moment of inertia of 12.45 ft^4. The location of the steel varies throughout the rib of the arch, with the major transition occurring at the quarter-span points (15'-0" from either end of the arch). At this point, the steel is bent from the arch rib's exterior to its interior. Several drawings indicate that the transition is not abrupt, so it is assumed that one third of the steel members change direction at the quarter-span points, with the remaining two thirds following thereafter.

Due to the small cross-sectional area of the steel, the transformed centroidal axis is approximately equal to the center of the concrete, with a span of 67'-0" and a height of 9.9'. The height-to-span ratio is approximately 1:6.8. Results of dead weight calculations are listed below (Table 12).

Table 12. Total weights of various materials in the West Union bridge.

Material	Weight (kips)
Concrete	1533.3
Spandrel Walls	51.5
Balustrades/Railing	190.5
Earth Fill	2825.8
Steel	3.7

Appendix B lists deflection, axial force, bending moment, and stress results for the second and third models under the uniform dead load condition. In general, displacements for all three models are extremely small. For the fixed-fixed condition, the arch displaces vertically a maximum of 0.105" at the crown under its own weight. With the added half-span live load of 100 psf, the vertical displacement at the crown is approximately 0.1194" with the maximum displacement occurring 1'-0" off center and totaling 0.1212". For the second model, the vertical displacement at the crown is 0.102" for the dead load condition. The tie displaces horizontally only 0.00312" at the support, while at the center it moves roughly 2.16". Under the live load condition, the vertical displacement at the center of the tie decreases to 1.992". Finally, the vertical displacement at the crown increases to 0.192" for the third model, while the displacement at the center of the tie decreases dramatically to 0.156".

For all three models, member forces are also calculated. For the dead load condition, the first two models reveal similar axial forces throughout the arch's length. The axial forces range from approximately -407 kips to -538 kips (negative numbers indicate compression). However, the axial forces in the third model are slightly smaller, -366 kips to -507 kips. The primary conclusion is that the Luten ties are effective for carrying horizontal thrust.

It is not possible to determine the exact cross-sectional properties used by Luten for this particular bridge. Several drawings of other structures designed by Luten indicate the presence of a lip at the tie's edges, which increases its cross-sectional area and moment of inertia, as in the third model.

Stresses in the first and second models are similar, with maximum compressive stresses occurring at the extrados of the crown and totaling approximately -0.330 ksi for concrete and -2.49 ksi for steel (negative numbers indicate compression). For the second model, the tie's steel has a relatively constant tensile stress of 3.3 ksi. Stresses for the third model indicate a slightly higher compressive stress at the center, totaling -0.406 ksi for concrete and -2.78 ksi for steel. These stresses also indicate that both the steel and the extrados of the concrete are in tension for the arch's first and last 15'-0", a verification of the steel's effective placement. The tensile stresses reach a maximum of 0.110 ksi for concrete and 0.395 ksi for steel. The tie's steel has a maximum tensile stress of 3.07 ksi. The magnitudes of all stresses computed are well within the capabilities of concrete and steel.

MARSH RAINBOW ARCH IN BOONE COUNTY, IOWA

There are several Marsh "rainbow arches" in Boone County, Iowa. The particular arch analyzed here has a span of 90'-0" and a total rise of 10'-6".[54] This single-span bridge with seven hangers was constructed in 1917. There are three major characteristics that distinguish this bridge from those designed by the Concrete-Steel Engineering Company and Luten: the open-spandrel configuration, the location of the arch rib above the deck, and the use of latticed-girder reinforcement within the arch rib and vertical members. One of the principal patent claims made by Marsh is for a slip joint between the deck and the arch where they intersect (section 7-7 in Figure 21). Therefore, Marsh did not want the deck to act as a tie, but rather to simply transfer loads to the vertical elements. He also did not want thermal changes in the deck's length to cause axial forces and moments in the arch.

The dominant loading condition for this arch is the distributed dead weight of the deck (3.6 kips/ft) and a parabolic thrust line is therefore used. The arch has a constant width of 21". The vertical members vary in height from 2'-0" near the junction of the arch rib and the deck to 8'-0" at the center. The rib contains four 3" angles arranged as shown in Figure 34. The vertical members' reinforcement is of a similar arrangement, using four 2" angles. The deck has a total width of 18'-0" and a thickness of 16".

For the structural analysis, the bridge is modeled as a plane frame with 48 members and 22 nodes (Figure 35). Unlike the Rock Rapids arch and the West Union arch models, each section consists of concrete and steel elements in parallel (due to the latticed-girder reinforcement). Under its distributed dead load, the arch's maximum vertical displacement of 0.163" occurs at node 10. With a half-span distributed live load of 1.8 kips/ft, the maximum vertical displacement of 0.203" also occurs at node 10 (Appendix C). The axial forces in the arch rib are maximum at the supports, -182.0 kips, and minimum at the crown, -169.0 kips (negative numbers indicate compression). Under the effects of the half-span live load, the axial force increases to -222.0 kips at the abutments and -194.0 kips at the crown. Tensile axial forces only exist in the vertical and deck members. Generally, these values are small, at least one order of magnitude less than the compressive forces in the arch rib (Appendix C).

Within the arch, maximum concrete stresses occurs near the supports, approximately -704 psi. Maximum tensile stresses of 193 psi exist within the concrete vertical members, and deck stresses range from 0 to 328 psi. Steel stresses within the vertical members are small with little variation, ranging from 19.85 psi to 41.18 psi.

SUMMARY

Melan, Emperger, Thacher, Mueser and their Concrete-Steel Engineering Company were important designers of turn-of-the-century American reinforced concrete arch bridges. They used approximate analysis to design primarily statically indeterminate, fixed-fixed, closed-spandrel arches. Modern analyses indicate that the working stresses in the arches are very low, probably contributing to their durability. Their continuous, centered I-beam and centered latticed-girder reinforcement do not rely on true composite action of steel and concrete and do not reflect the direction of bending moment at any section in the arch. The reinforcement systems patented later by Thacher show he understood that if concrete and steel are perfectly bonded or interlocked, lacing is not needed.

Luten designed effective reinforced concrete tied arches. His reinforcement systems are based on the assumption of true composite behavior of steel and concrete. His positioning of principal reinforcement near the intrados and extrados (Figure 20) reflects the direction of bending moment at any cross section. The West Union bridge is a beautiful, durable example of his work. Modern structural analyses again show very low working stresses.

Marsh's open-spandrel "rainbow arch" exemplifies the evolution of reinforced concrete bridge design away from filled-spandrel forms. The much greater rise-to-span ratio produces extremely stiff bridges. The latticed-girder reinforcement is a throwback to the Emperger system, and does not take advantage of the potential composite behavior of steel with concrete. However, the stiffness of the reinforcement may have been used to decrease the size and stiffness of the formwork required.

Each of the three arches studied are very successful structural designs, providing durable, safe bridges. The designs are based on approximate analyses of arches. Both Emperger and Marsh arches simply use steel in parallel with concrete, without relying on the bonding between steel and concrete or on true composite behavior. Only the Luten arch reflects reliance on composite behavior and an understanding of how bending moments vary along the arch's span.

GLOSSARY OF TERMS

Axial Force. A force in the direction of an element's axis.

Bending Moment. A force times the perpendicular distance to a point, with dimensions of force times length.

Composite Material. Two materials (e.g., concrete and steel) perfectly bonded so they act together and have the same strains.

Fixed-Fixed Arch. An arch with zero vertical, horizontal and rotational displacement at its two supports.

Free-Body Diagram. A figure that shows all of the forces acting on a body.

Model. A mathematical representation of a structure or load.

Modulus of Elasticity. A material constant that relates the normal stress on a material to the normal strain. In other words, stress is the modulus of elasticity times strain.

Moment of Inertia. The geometric property of a cross-section that controls the stresses from a bending moment. For a rectangular section of depth, *a,* and width, *b,* the moment of inertia is equal to $ba^3/12$.

Normal Strain. The change in an element's length divided by its original length.

Normal Stress. Force per unit area.

Section Modulus. A section's moment of inertia divided by the distance from the centroid to the surface. For a rectangular section, the section modulus is equal to $ba^2/6$.

Shear. A force perpendicular to the axis of an element.

Statically Determinate Structure. A structure whose interior forces may be determined completely from only force equilibrium equations.

Statically Indeterminate Structure. A structure whose interior forces cannot be determined completely from *only* force equilibrium equations. Interior forces can be determined if other equations are also used.

Tensile Strength. The normal stress that will cause tensile rupture in a material.

ENDNOTES

1. Robert E. Loov, "Reinforced Concrete at the Turn of the Century," *Concrete International,* vol. 13, no. 12 (December 1991): 67.

2. Ibid.

3. Ibid.

4. Ibid.

5. Ibid.

6. Ibid.

7. Edwin Thacher, "Concrete and Concrete-Steel in the United States," *Transactions of the American Society of Civil Engineers,* vol. 54, pt. E (1905): 437.

8. Loov, "Reinforced Concrete at the Turn of the Century".

9. Jacques Heyman, *Coulomb's Memoir on Statics* (Cambridge: Cambridge UP, 1972). William Addis, *Structural Engineering: The Nature of Theory and Design* (New York: Ellis Horwood, 1990).

10. Joseph Melan, *Plain and Reinforced Concrete Arches,* trans. D. B. Steinman (New York: Wiley, 1915). Malverd Howe, *A Treatise on Arches* (New York: Wiley, 1897). Joseph Balet, *Analysis of Elastic Arches* (New York: Engineering News Publishing, 1908).

11. Siegfried Giedion, *Space, Time and Architecture* (Cambridge, Massachusetts: Harvard UP, 1967).

12. Friedrich von Emperger, "Concrete-Steel Bridges," *Transactions of the American Society of Civil Engineers,* vol. 54, pt. E (1905): 525.

13. Daniel B. Luten, "The Proper Curvature for a Filled Spandrel Arch," *Railroad Gazette,* September 12, 1902. Howe, *A Treatise on Arches.*

14. Loov, "Reinforced Concrete at the Turn of the Century".

15. Steven H. Kosmatka and William C. Panarese, *Design and Control of Concrete Mixtures* (Illinois: Portland Cement Association, 1988).

16. Thacher, "Concrete and Concrete-Steel," p. 425.

19. Friedrich von Emperger, "Melan Concrete Arch of 100' Span, Stockbridge Massachusetts," *Engineering News,* November 7, 1895.

20. John S. Sewell, "Concrete and Concrete-Steel in the United States," *Transactions of the American Society of Civil Engineers,* vol. 54, pt. E (1905): 462.

21. Ibid., p. 476.

22. Friedrich von Emperger, "The Development and Recent Improvement of Concrete-Iron Highway Bridges," *Transactions of the American Society of Civil Engineers* vol. 31 (1894): 447, 450.

23. F. E. Turneaure and E. R. Maurer, *Principles of Reinforced Concrete Construction* (New York: Wiley, 1908).

24. Ibid.

25. Emperger, "The Development and Recent Improvement of Concrete-Iron Highway Bridges," and "Concrete-Steel Bridges".

26. Homer Reid, *Concrete and Reinforced Concrete Construction*, (New York: Myron C. Clark, 1907). Albert W. Buel and Charles Hill, *Reinforced Concrete*, (New York: Engineering News Publishing, 1906). Turneaure and Maurer, *Principles of Reinforced Concrete Construction.* F. W. Taylor and S. E. Thompson, *Treatise of Concrete Plain and Reinforced,* (New York: Wiley, 1907). Howe, *A Treatise on Arches.* Armand Considere, *Experimental Researches on Reinforced Concrete,* 2nd ed., trans. Leon Moisseiff (New York: McGraw-Hill, 1906). Emil Morsch, *Concrete-Steel Construction,* trans. E. P. Goodrich (New York: Engineering News Publishing, 1909).

27. Buel and Hill, *Reinforced Concrete.*

28. Joseph Melan, "Vault for Ceilings, Bridges, Etc.," U.S. Patent No. 505,054 (1893).

29. Friedrich von Emperger, "Vault for Ceilings, Bridges, Etc.," U.S. Patent No. 583,464 (1897).

30. Edwin Thacher, "Concrete Arch," U.S. Patent No. 617,615 (1899).

31. Ibid.

32. Personal correspondence with the biographer, Jim Cooper, 629 East Seminar Street, Greencastle, Indiana 46135.

34. Luten, "The Proper Curvature for a Filled Spandrel Arch".

35. Joseph Snyder and Steve Mikesell, "The Consulting Engineer and Early Concrete Bridges in California," *Concrete International,* May 1994, pp. 38-44.

36. Ibid.

37. Ibid.

38. James B. Marsh, "Reinforced Arch Bridge," U.S. Patent No. 1,035,026 (August 6, 1912).

39. Clyde T. Morris, "Concrete and Reinforced Concrete Arches: Final Report of the Special Committee," *Transactions of the American Society of Civil Engineers*, vol. 100 (1935): 1429.

40. Emperger, "The Development and Recent Improvement of Concrete-Iron Highway Bridges," p. 447.

41. Ibid., p. 453.

42. Carl Gayler, "Discussion," *Transactions of the American Society of Civil Engineers,* vol. 31 (1894): 469.

43. Bernt Berger, "Discussion," *Transactions of the American Society of Civil Engineers,* vol. 31 (1894): 471.

44. Ibid.

45. Kosmatka and Panarese, *Design and Control of Concrete Mixtures.*

46. W. R. Hutton, "Discussion," *Transactions of the American Society of Civil Engineers,* vol. 31 (1894): 473.

47. U.S. Department of the Interior, Historic American Engineering Record (HAER), No. IA-15, "Melan Arch Bridge," 1985, p. 5, Prints and Photographs Division, Library of Congress, Washington, D.C.

48. Ibid., p. 6.

49. Ibid., p. 7.

50. Ibid.

51. Edwin Thacher, "Concrete and Concrete-Steel in the United States," p. 439.

53. Luten, "The Proper Curvature for a Filled Arch".

54. Clayton B. Fraser, HAER Inventory Card, "Beaver Creek Bridge" (BOON07, FHWA 077250), *Iowa Historic Bridge Inventory* (Ames, Iowa: Iowa Department of Transportation, 1994).

SOURCES CONSULTED

Addis, William. *Structural Engineering: The Nature of Theory and Design.* New York: Ellis Horwood, 1990.

Balet, Joseph. *Analysis of Elastic Arches.* New York: Engineering News Publishing, 1908.

Berger, Bernt. "Discussion." *Transactions of the American Society of Civil Engineers,* vol. 31 (1894).

Buel, Albert W., and Charles Hill. *Reinforced Concrete.* New York: Engineering News Publishing, 1906.

Considere, Armand. *Experimental Researches on Reinforced Concrete.* 2nd ed. Trans. Leon Moisseff. New York: McGraw-Hill, 1906.

Cooper, Jim. Personal correspondence with author.

Emperger, Friedrich von. "Concrete-Steel Bridges." *Transactions of the American Society of Civil Engineers,* vol. 54, pt. E (1905).

_____. "The Development and Recent Improvement of Concrete-Iron Highway Bridges." *Transactions of the American Society of Civil Engineers,* vol. 31 (1894).

_____. "Melan Concrete Arch of 100' Span, Stockbridge, Massachusetts." *Engineering News,* November 7, 1895.

_____. "Vault for Ceilings, Bridges, Etc." U.S. Patent No. 583,464 (1897).

Fraser, Clayton B. HAER Inventory Card, "Beaver Creek Bridge" (BOON08, FHWA 077250). *Iowa Historic Bridge Inventory.* Ames, Iowa: Iowa Department of Transportation, 1994.

Gayler, Carl. "Discussion." *Transactions of the American Society of Civil Engineers,* vol. 31 (1894).

Giedion, Siegfried. *Space, Time and Architecture.* Cambridge, Massachusetts: Harvard UP, 1967.

Heyman, Jacques. *Coulomb's Memoir on Statics.* Cambridge: Cambridge UP, 1972.

Howe, Malverd. *A Treatise on Arches.* New York: Wiley, 1897.

Hutton, W. R. "Discussion." *Transactions of the American Society of Civil Engineers,* vol. 31 (1894).

Kosmatka, Steven H., and William C. Panarese. *Design and Control of Concrete Mixtures.* Illinois: Portland Cement Association, 1988.

Loov, Robert E. "Reinforced Concrete at the Turn of the Century." *Concrete International,* vol. 13, no. 12 (December 1991).

Luten, Daniel B. "The Proper Curvature for a Filled Spandrel Arch." *Railroad Gazette,* September 12, 1902.

Marsh, James B. "Reinforced Arch Bridge." U.S. Patent No. 1,035,026 (August 6, 1912).

Melan, Joseph. *Plain and Reinforced Concrete Arches.* Trans. D. B. Steinman. New York: Wiley, 1915.

_____. "Vault for Ceilings, Bridges, Etc." U.S. Patent No. 505,054 (1893).

Morris, Clyde T. "Concrete and Reinforced Concrete Arches: Final Report of the Special Committee." *Transactions of the American Society of Civil Engineers,* vol. 100 (1935).

Morsch, Emil. *Concrete-Steel Construction.* Trans. E. P. Goodrich. New York: Engineering News Publishing, 1909.

Reid, Homer. *Concrete and Reinforced Concrete Construction.* New York: Myron C. Clark, 1907.

Sewell, John S. "Concrete and Concrete-Steel in the United States." *Transactions of the American Society of Civil Engineers,* vol. 54, pt. E (1905).

Simmons, David. "Pioneer Concrete Arch Bridge Remains in Dayton." *Ohio County Engineer,* Fall 1993, pp. 10-11.

Snyder, Joseph, and Steve Mikesell, "The Consulting Engineer and Early Concrete Bridges in California," *Concrete International,* May 1994, pp. 38-44.

Taylor, F. W., and S. E. Thompson. *Treatise of Concrete Plain and Reinforced.* New York: Wiley, 1907.

Thacher, Edwin. "Concrete and Concrete-Steel in the United States." *Transactions of the American Society of Civil Engineers,* vol. 54, pt. E (1905).

_____. "Concrete Arch." U.S. Patent No. 617,615 (1899).

Turneaure, F. E., and E. R. Maurer. *Principles of Reinforced Concrete Construction.* New York: Wiley, 1908.

U.S. Department of the Interior, Historic American Engineering Record (HAER), No. IA-15, "Melan Arch Bridge," 1985. Prints and Photographs Division, Library of Congress, Washington, D.C.

_____, No. IA-53, "Twin Bridge," 1995. Prints and Photographs Division, Library of Congress, Washington, D.C.

FIGURES

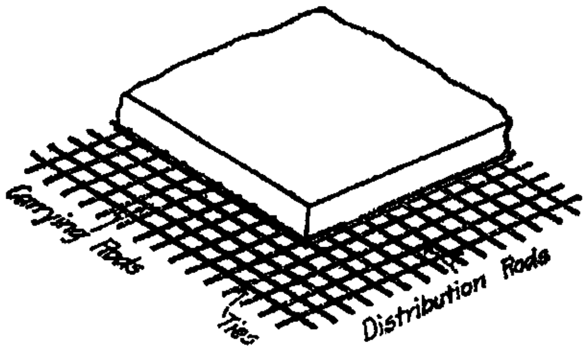

Figure 1. Monier trellis. Illustration from Homer Reid, *Concrete and Reinforced Concrete Construction* (New York: Myron C. Clark, 1907).

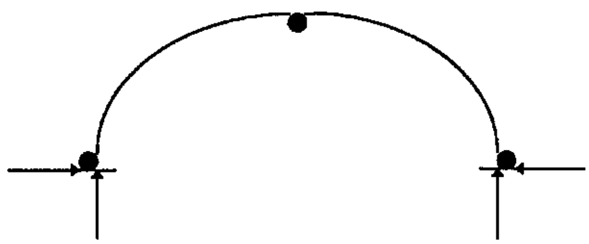

Figure 2. Three-hinged arch. Arrows represent reaction forces, and circles represent hinges.

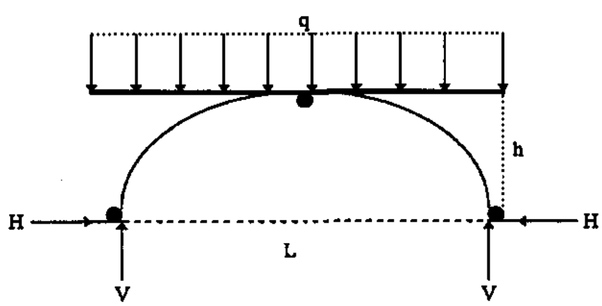

Figure 3. Three-hinged arch with vertical distributed loading.

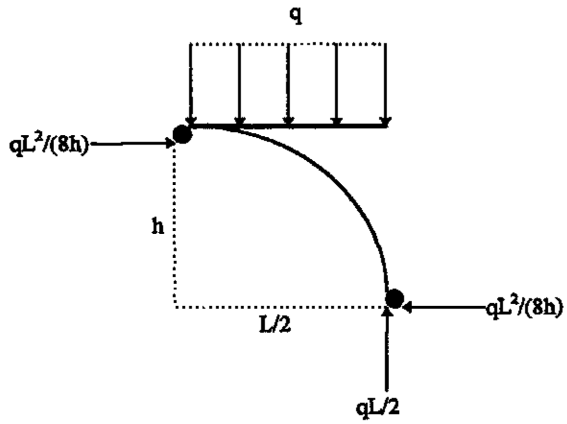

Figure 4. Free-body diagram of a three-hinged arch.

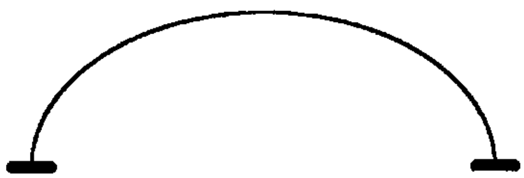

Figure 5. Fixed-fixed arch.

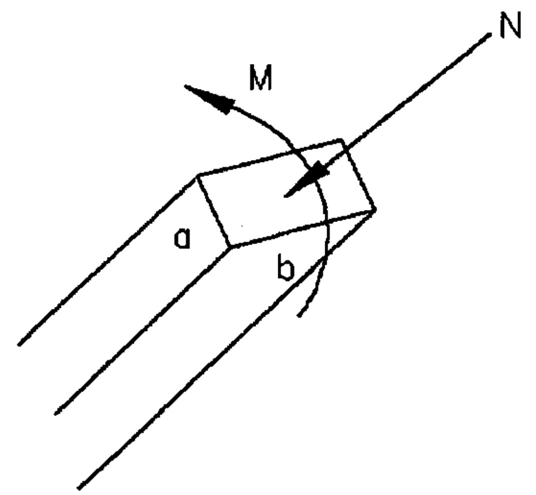

Figure 6. Arch cross section.

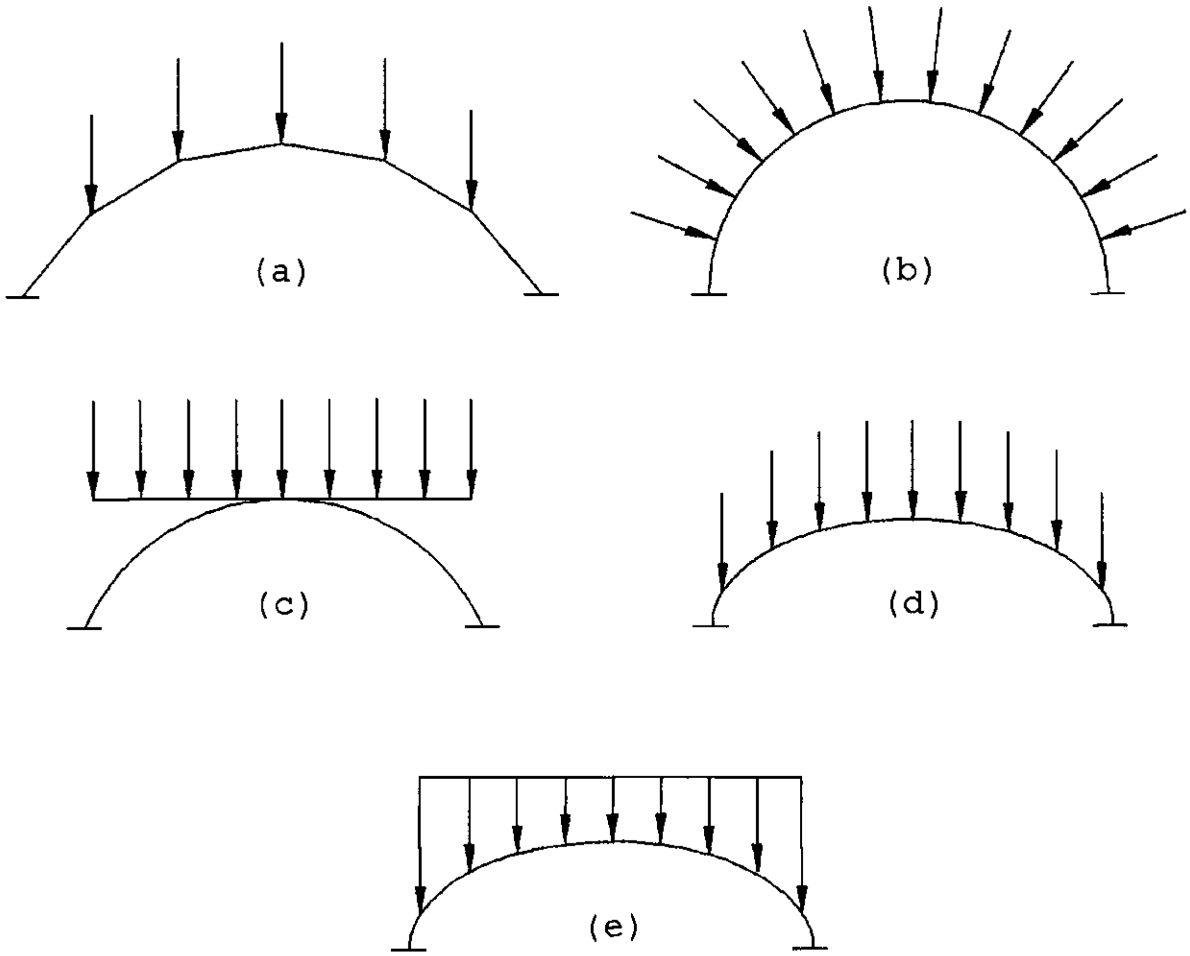

Figure 7. Thrust lines for common arch load conditions. (a) Piecewise linear arch. (b) Circular arch with distributed loading normal to arch axis. (c) Parabolic arch with vertical loading distributed along horizontal projection. (d) Catenary with vertical loading distributed along arch axis. (e) Transformed catenary with vertical distributed loading varying with the distance between the arch axis and a horizontal line above it.

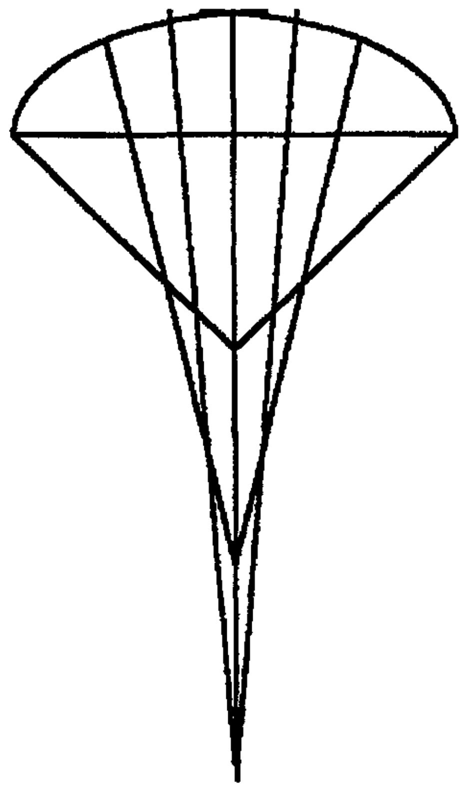

Figure 8. Three-centered arch.

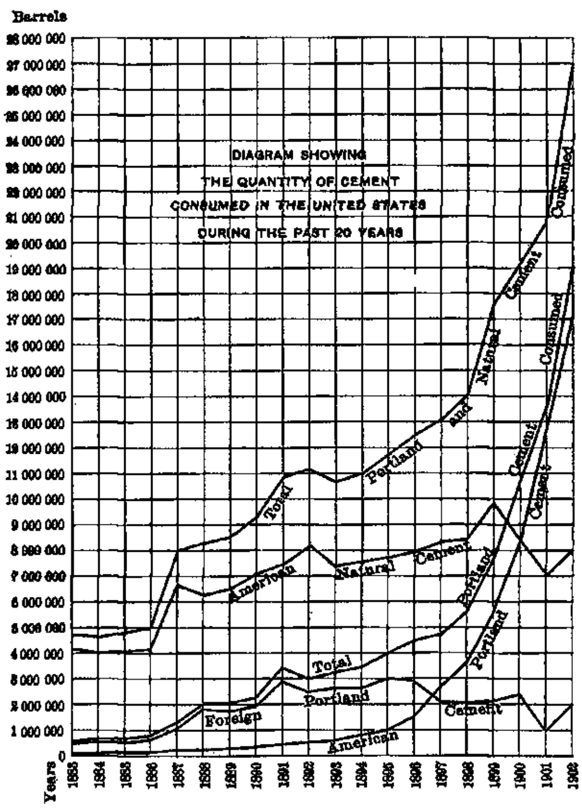

FIG. 1.

Figure 9. Graph showing cement consumption during the years 1893-1902. Illustration from Edwin Thacher, "Concrete and Concrete-Steel in America," *Transactions of the American Society of Civil Engineers,* vol. 54, pt. E (1905): 427.

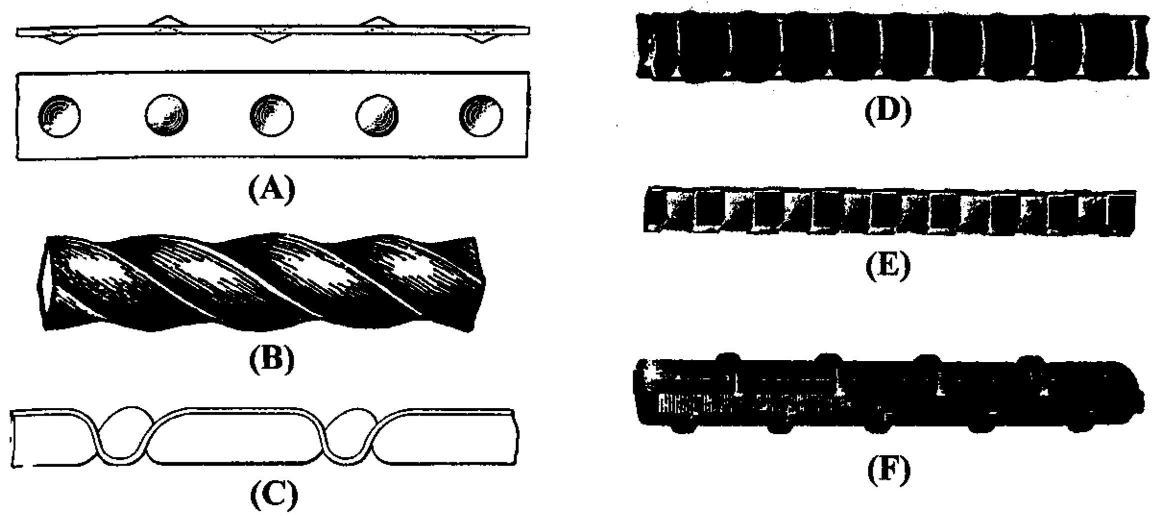

Figure 10. Early reinforcing bars. (A) Staff bar. (B) Ransome bar. (C) De Man crimped bar. (D) Cup bar. Illustrations from Homer Reid, *Concrete and Reinforced Concrete Construction* (New York: Myron C. Clark, 1907). (E) Corrugated square bar. Illustration from F. W. Taylor and S. E. Thompson, *Treatise of Concrete Plain and Reinforced* (New York: Wiley, 1907). (F) Corrugated round bar. Illustration from Corrugated Bar Company, *Useful Data* (Buffalo: Corrugated Bar Company, 1919).

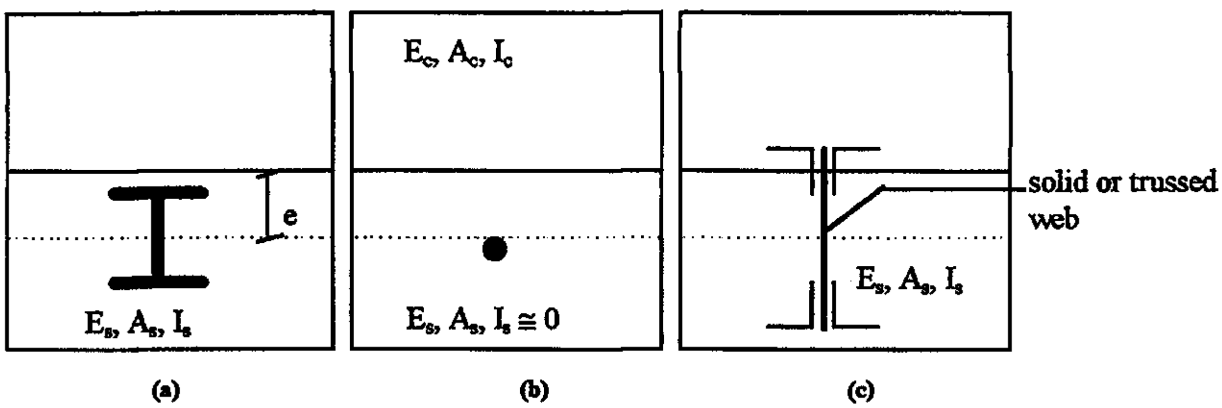

Figure 11. Reinforced concrete sections, where centroidal axes of concrete and steel are separated by eccentricity, *e*.

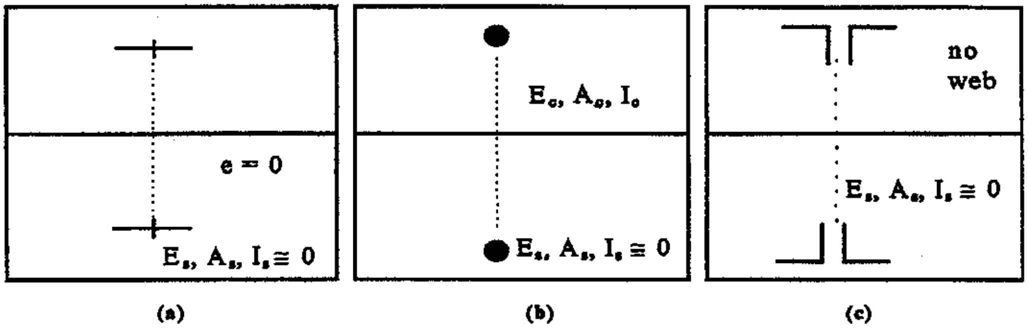

Figure 12. Reinforced concrete sections, where centroidal axes of concrete and steel coincide (Thacher type reinforcement).

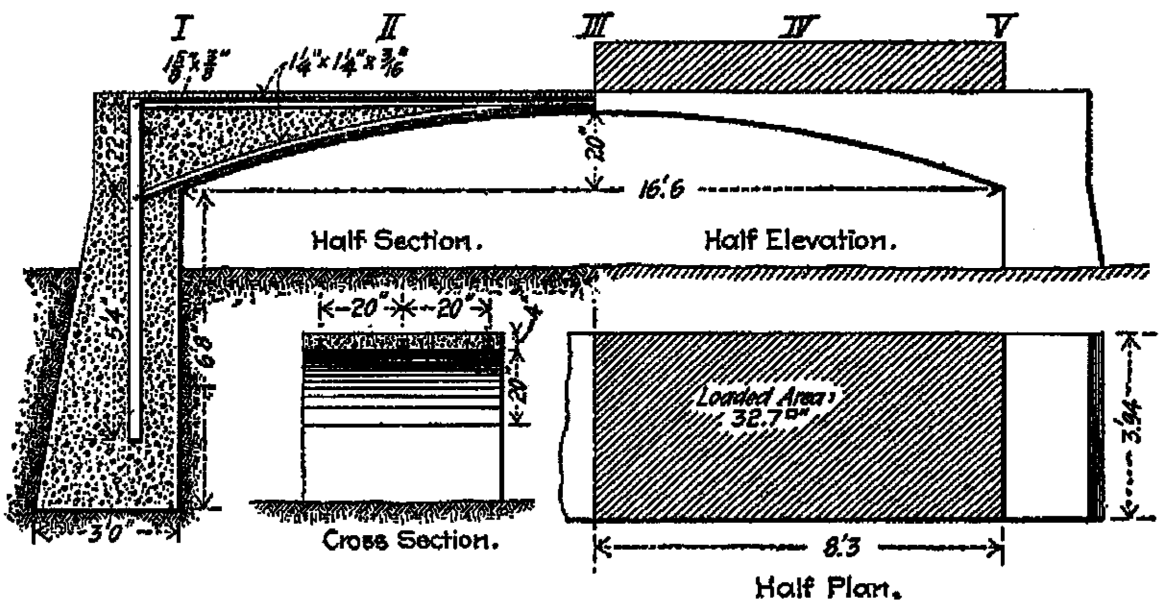

FIG. 3.

Figure 13. Reinforcing system used by Wünsch. Illustration from Friedrich von Emperger, "The Development and Recent Improvement of Concrete-Iron Highway Bridges," *Transactions of the American Society of Civil Engineers,* vol. 31 (1894): 443.

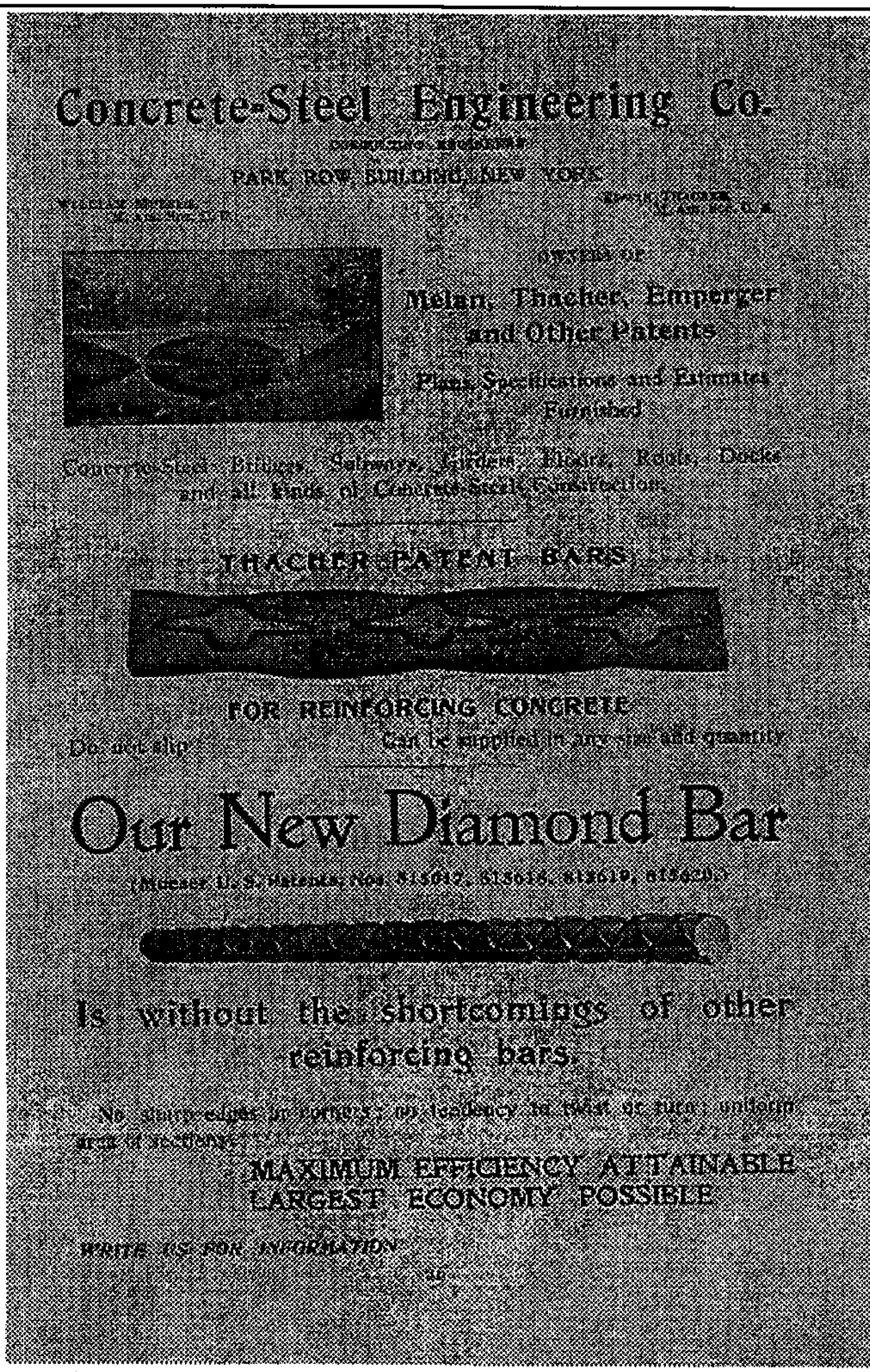

Figure 14. Advertisement for the Concrete-Steel Engineering Company. Illustration from Homer Reid,

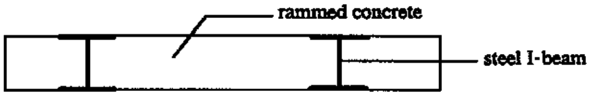

Figure 15. Cross section of Melan's 1893 prismatic arch.

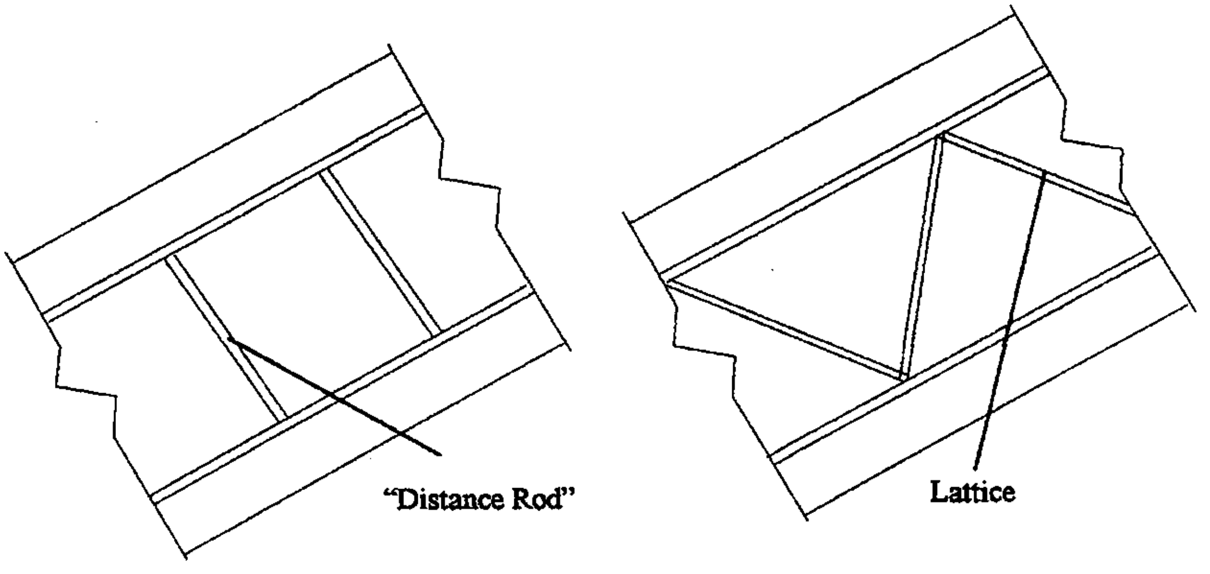

Figure 16. Reinforcing systems patented by Emperger in 1897.

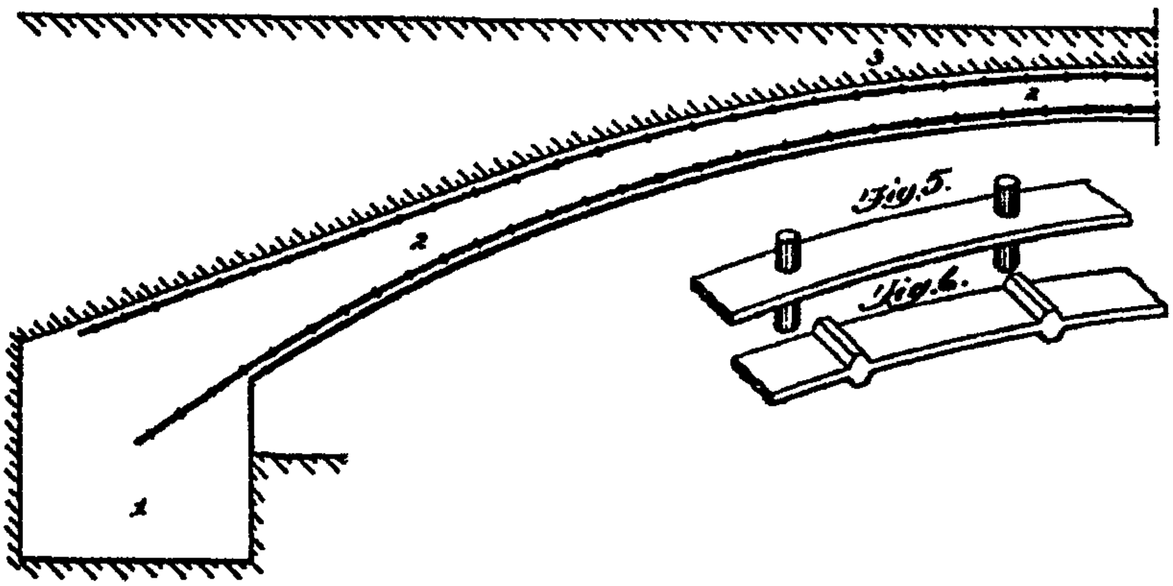

Figure 17. Reinforcing bars patented by Thacher in 1899. Illustration from Edwin Thacher, "Concrete Arch," U.S. Patent No. 617,615 (1899).

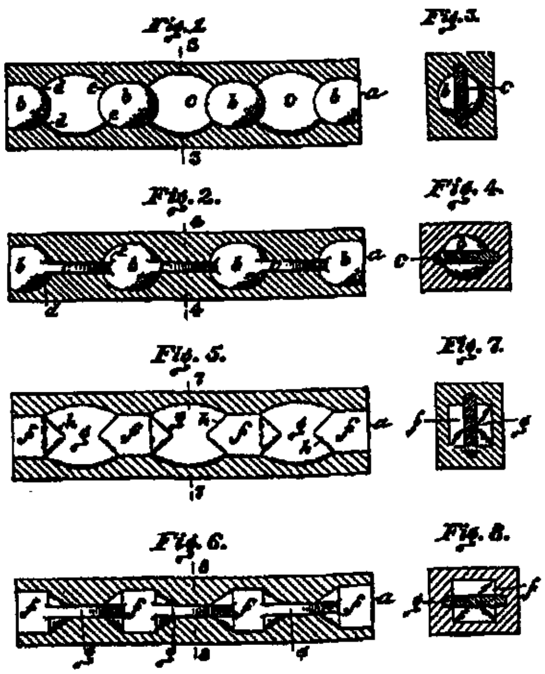

Figure 18. Reinforcing bars patented by Thacher in 1902.

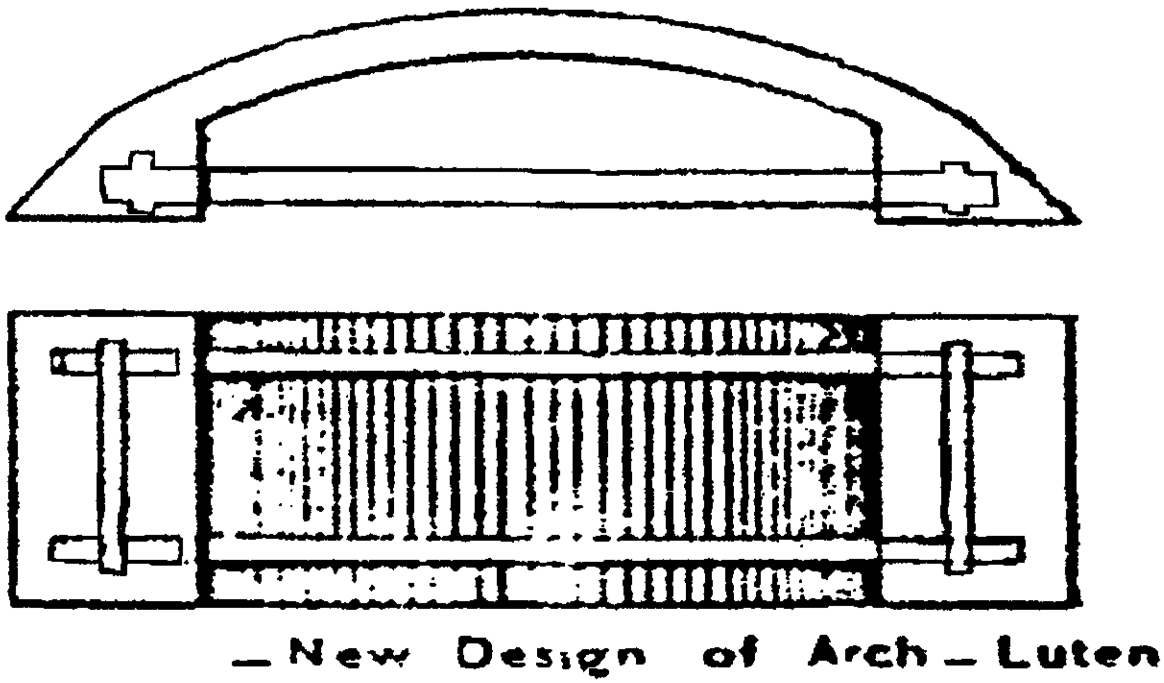

Figure 19. Luten's closed-spandrel timber-tied arch.

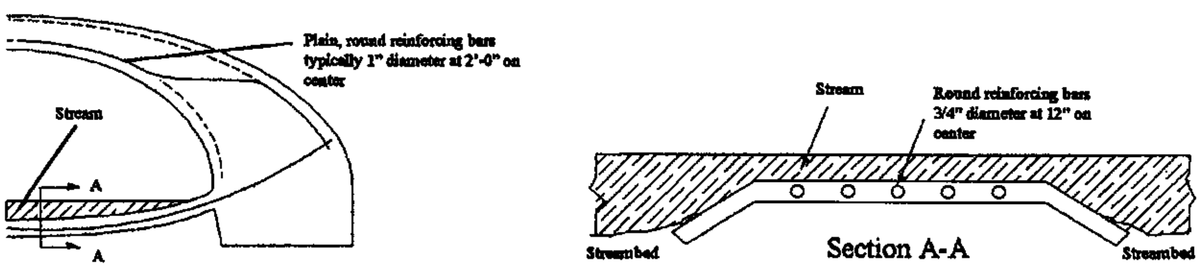

Figure 20. Luten's 1902 tied arch uses a reinforced concrete tie.

J. B. MARSH.
REINFORCED ARCH BRIDGE.
APPLICATION FILED NOV. 1, 1911.

1,035,026.

Patented Aug. 6, 1912.
4 SHEETS—SHEET 1.

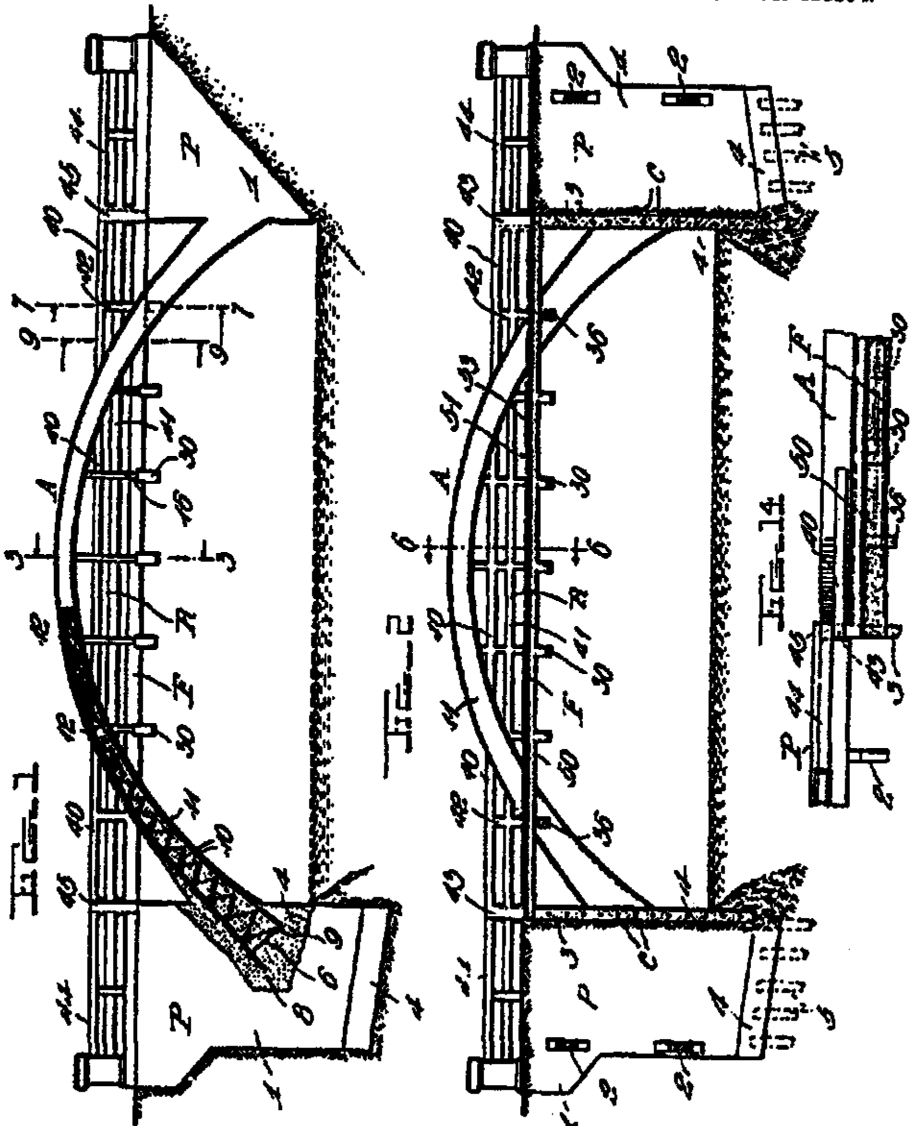

Witnesses

N. L. Collamer

Inventor
J. B. Marsh
by H. B. Willson & Co
Attorneys

Figure 21. Open-spandrel reinforced concrete arch. Illustration from James B. Marsh, "Reinforced Arch

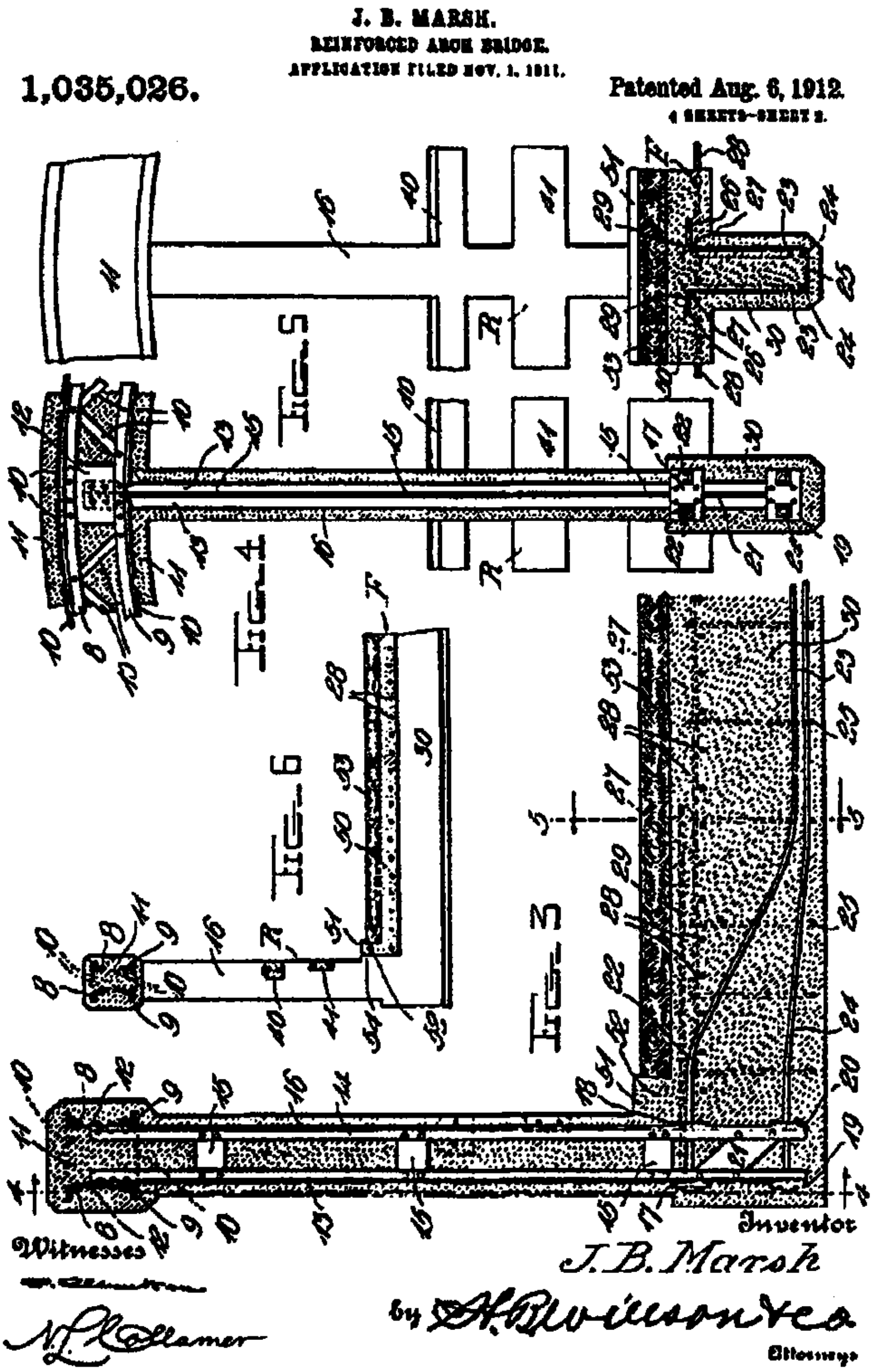

Figure 22. Open-spandrel reinforced concrete arch. Illustration from James B. Marsh, "Reinforced Arch Bridge," U.S. Patent No. 1,035,026 (August 6, 1912).

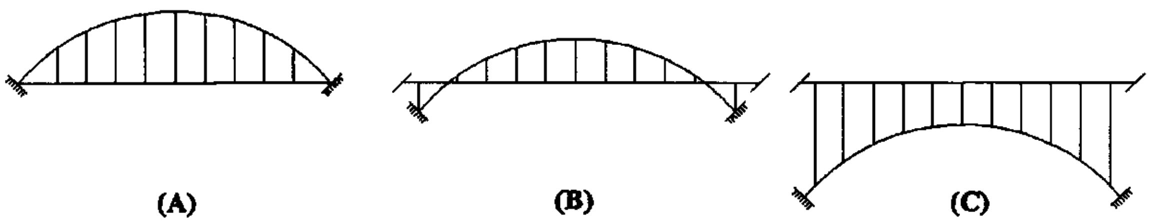

Figure 23. The open-spandrel arch is adaptable to a variety of topographic conditions.

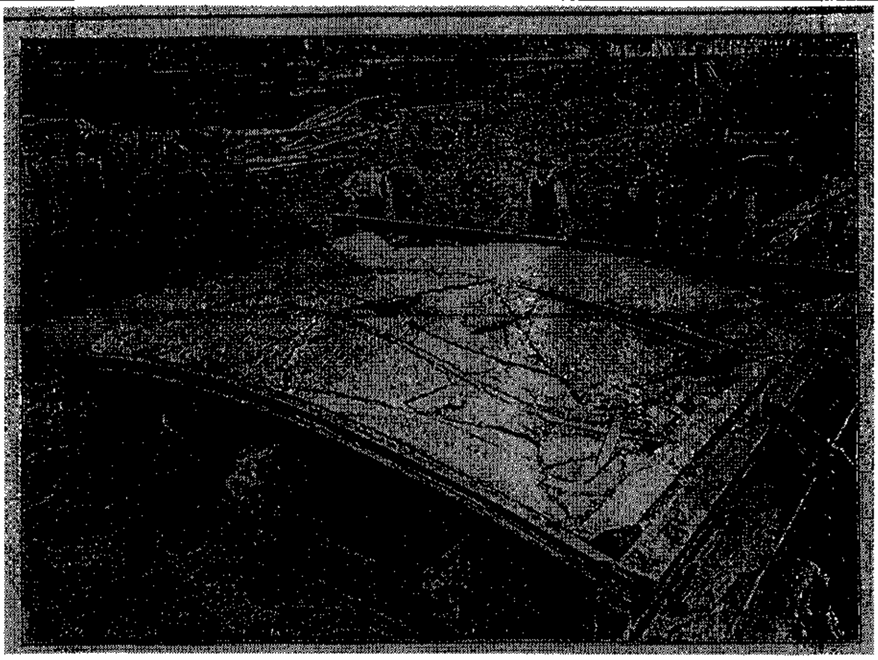

Figure 24. Melan arch tested by the Austrian Society of Engineers and Architects. Illustration from Friedrich von Emperger, "The Development and Recent Improvement of Concrete-Iron Highway Bridges," *Transactions of the American Society of Civil Engineers,* vol. 31 (1894): opp. 448.

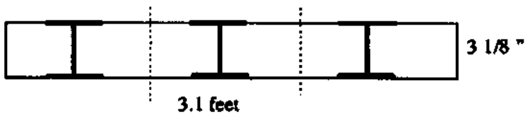

Figure 25. Cross section through Melan arch.

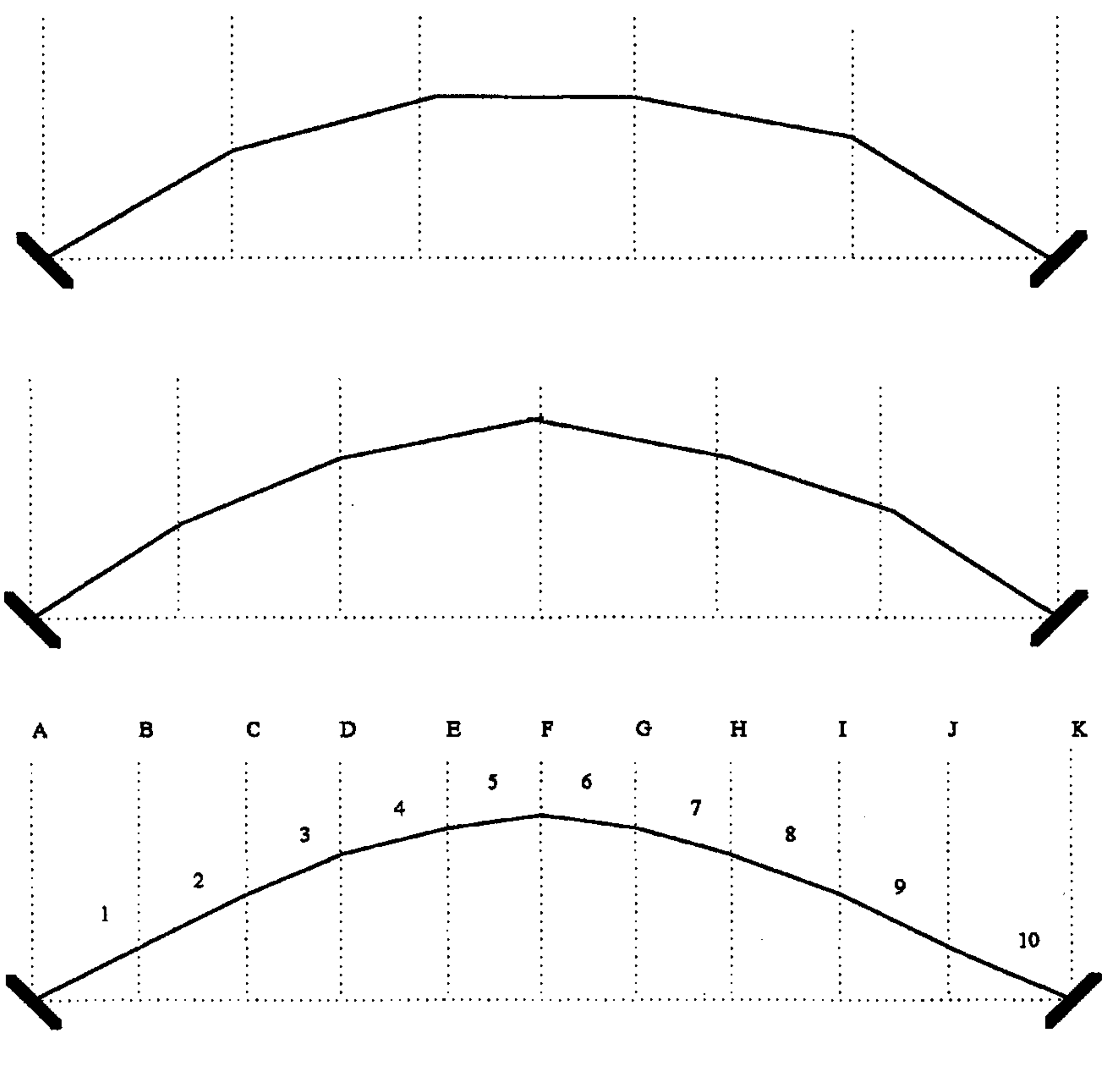

Figure 26. Arch modeled with straight segments. Numbers denote beam members, letters denote sections.

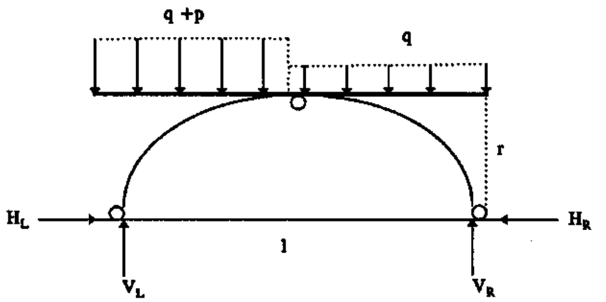

Figure 27. Three-hinged arch with vertical distributed dead load on entire span, plus half-span live load.

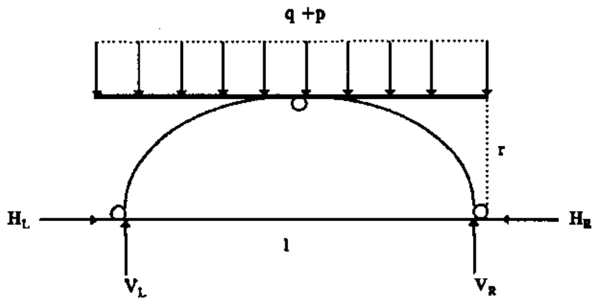

Figure 28. Three-hinged arch with vertical distributed loading on entire span, plus full-span live load.

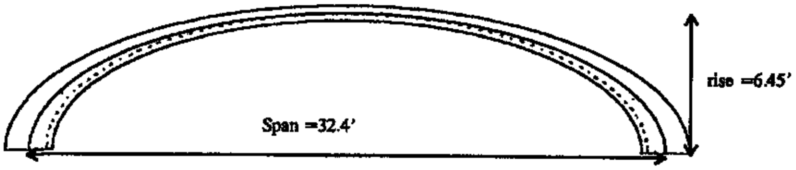

Figure 29. Melan's Rock Rapids arch with transformed centroidal axis. Dotted line represents the steel centroidal axis location.

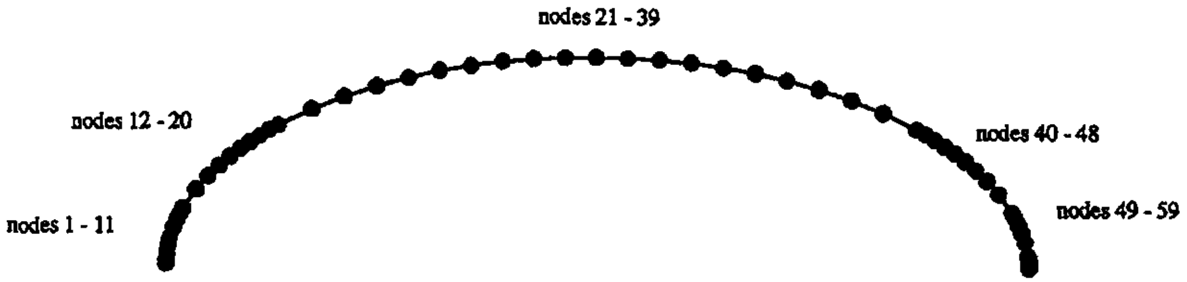

Figure 30. Melan arch modeled as a 58-member plane frame. Circles represent nodal coordinates.

Figure 31. Cross section of concrete tie without lip.

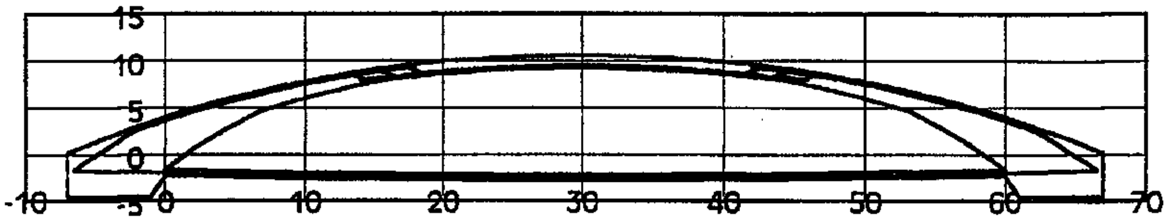

Figure 32. Luten's West Union arch (coordinates in feet).

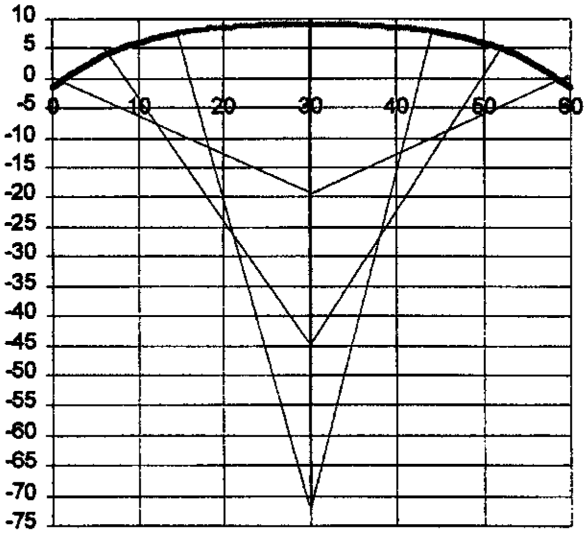

Figure 33. Three-centered arch intrados (coordinates in feet).

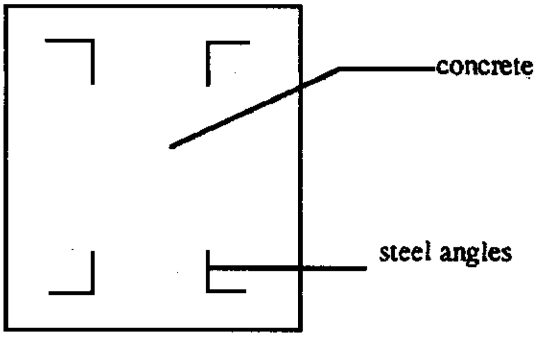

Figure 34. Section through Marsh's Boone County arch rib.

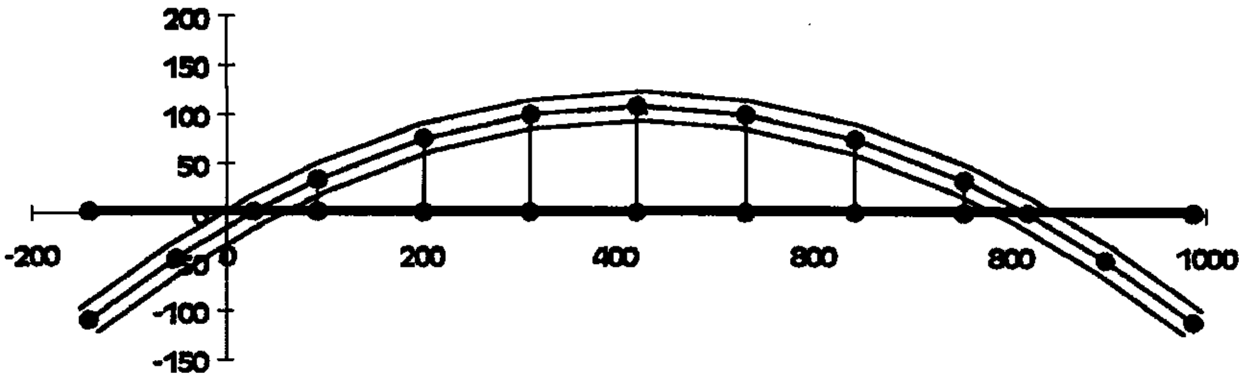

Figure 35. Marsh arch modeled as a 23-node, 48-member plane frame (coordinates in inches).

APPENDIX A: MELAN-EMPERGER ARCH

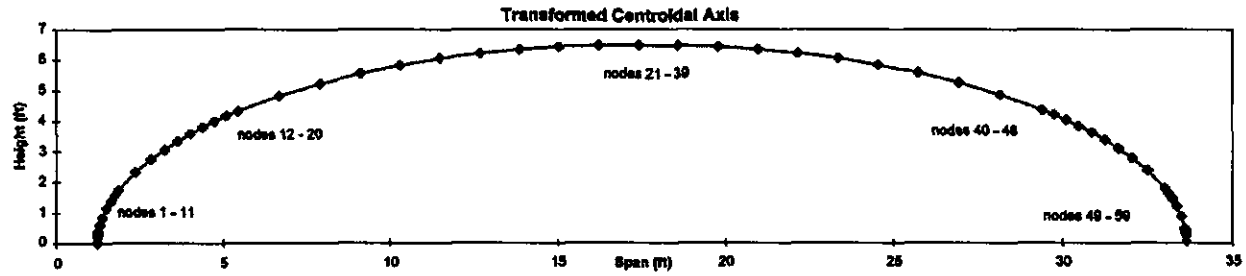

Table A-1. Geometric Section Properties of Melan-Emperger Arch.

Node no.	Rib thickness (ft)	Concrete area (ft²)	Steel area (ft²)	Concrete moment of inertia (ft⁴)	Steel moment of Inertia (ft⁴)	Node no.	Rib thickness (ft)	Concrete area (ft²)	Steel area (ft²)	Concrete moment of Inertia (ft⁴)	Steel moment of Inertia (ft⁴)
1	7.37e-01	6.74e-01	8.53e-04	3.05e-02	1.71e-06	31	2.13e-01	1.95e-01	8.53e-04	7.38e-04	1.71e-06
2	7.35e-01	6.72e-01	8.53e-04	3.03e-02	1.71e-06	32	2.16e-01	1.97e-01	8.53e-04	7.66e-04	1.71e-06
3	7.33e-01	6.71e-01	8.53e-04	3.00e-02	1.71e-06	33	2.21e-01	2.02e-01	8.53e-04	8.18e-04	1.71e-06
4	7.32e-01	6.69e-01	8.53e-04	2.98e-02	1.71e-06	34	2.27e-01	2.08e-01	8.53e-04	8.97e-04	1.71e-06
5	7.30e-01	6.68e-01	8.53e-04	2.97e-02	1.71e-08	35	2.37e-01	2.17e-01	8.53e-04	1.01e-03	1.71e-06
6	7.21e-01	6.59e-01	8.53e-04	2.85e-02	1.71e-06	36	2.49e-01	2.28e-01	8.53e-04	1.18e-03	1.71e-06
7	7.06e-01	6.46e-01	8.53e-04	2.68e-02	1.71e-06	37	2.65e-01	2.42e-01	8.53e-04	1.42e-03	1.71e-06
8	6.80e-01	8.22e-01	8.53e-04	2.39e-02	1.71e-06	38	2.86e-01	2.61e-01	8.53e-04	1.78e-03	1.71e-06
9	6.57e-01	6.01e-01	8.53e-04	2.18e-02	1.71e-06	39	3.13e-01	2.87e-01	8.53e-04	2.34e-03	1.71e-06
10	6.37e-01	5.82e-01	8.53e-04	1.97e-02	1.71e-06	40	3.51e-01	3.21e-01	8.53e-04	3.30e-03	1.71e-06
11	6.19e-01	5.68e-01	8.53e-04	1.81e-02	1.71e-06	41	3.65e-01	3.33e-01	8.53e-04	3.69e-03	1.71e-06
12	5.51e-01	5.04e-01	8.53e-04	1.27e-02	1.71e-06	42	3.80e-01	3.47e-01	8.53e-04	4.17e-03	1.71e-06
13	5.04e-01	4.61e-01	8.53e-04	9.74e-03	1.71e-06	43	3.97e-01	3.63e-01	8.53e-04	4.76e-03	1.71e-06
14	4.68e-01	4.28e-01	8.53e-04	7.83e-03	1.71e-06	44	4.17e-01	3.81e-01	8.53e-04	5.51e-03	1.71e-06
15	4.40e-01	4.02e-01	8.53e-04	6.49e-03	1.71e-06	45	4.40e-01	4.02e-01	8.53e-04	6.49e-03	1.71e-06
16	4.17e-01	3.81e-01	8.53e-04	5.51e-03	1.71e-06	46	4.68e-01	4.28e-01	8.53e-04	7.83e-03	1.71e-08
17	3.97e-01	3.63e-01	8.53e-04	4.76e-03	1.71e-06	47	5.04e-01	4.61e-01	8.53e-04	9.74e-03	1.71e-06
18	3.80e-01	3.47e-01	8.53e-04	4.17e-03	1.71e-06	48	5.51e-01	5.04e-01	8.53e-04	1.27e-02	1.71e-06
19	3.65e-01	3.33e-01	8.53e-04	3.69e-03	1.71e-06	49	6.19e-01	5.66e-01	8.53e-04	1.81e-02	1.71e-06
20	3.51e-01	3.21e-01	8.53e-04	3.30e-03	1.71e-06	50	6.37e-01	5.82e-01	8.53e-04	1.97e-02	1.71e-06
21	3.13e-01	2.87e-01	8.53e-04	2.34e-03	1.71e-06	51	6.57e-01	6.01e-01	8.53e-04	2.16e-02	1.71e-06
22	2.86e-01	2.61e-01	8.53e-04	1.78e-03	1.71e-06	52	6.80e-01	6.22e-01	8.53e-04	2.39e-02	1.71e-06
23	2.65e-01	2.42e-01	8.53e-04	1.42e-03	1.71e-06	53	7.06e-01	6.46e-01	8.53e-04	2.88e-02	1.71e-06
24	2.49e-01	2.28e-01	8.53e-04	1.18e-03	1.71e-06	54	7.28e-01	6.66e-01	8.53e-04	2.95e-02	1.71e-06
25	2.37e-01	2.17e-01	8.53e-04	1.01e-03	1.71e-06	55	7.30e-01	6.68e-01	8.53e-04	2.97e-02	1.71e-06
28	2.27e-01	2.08e-01	8.53e-04	8.97e-04	1.71e-06	56	7.32e-01	6.69e-01	8.53e-04	2.98e-02	1.71e-06
27	2.21e-01	2.02e-01	8.53e-04	8.18e-04	1.71e-06	57	7.33e-01	6.71e-01	8.53e-04	3.00e-02	1.71e-06
28	2.16e-01	1.97e-01	8.53e-04	7.66e-04	1.71e-08	58	7.35e-01	8.72e-01	8.53e-04	3.03e-02	1.71e-06
29	2.13e-01	1.95e-01	8.53e-04	7.36e-04	1.71e-06	59	7.37e-01	6.74e-01	8.53e-04	3.05e-02	1.71e-06
30	2.12e-01	1.94e-01	8.53e-04	7.26e-04	1.71e-06						

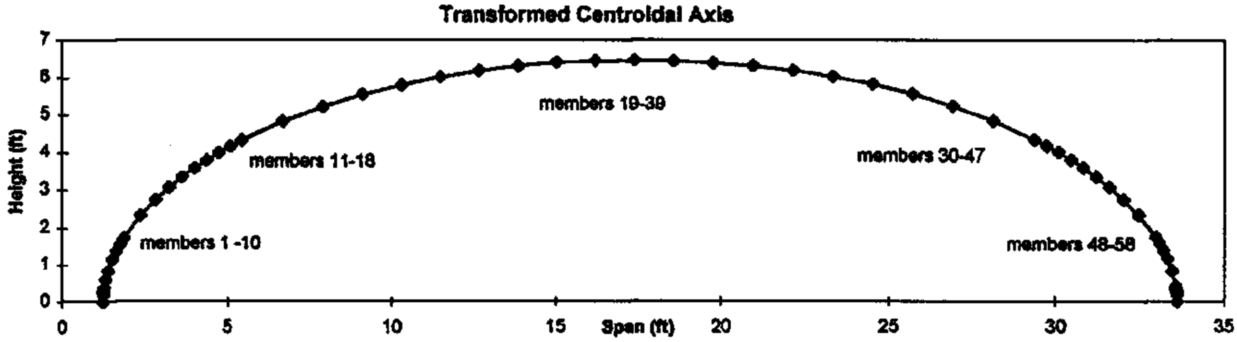

Table A-2. Member Forces in Melan-Emperger Arch (dead load).

Member no.	Bending moment (i) (kip-in)	Bending Moment (j) (kip-in)	Axial force (kips)	Member no.	Bending moment (i) (kip-in)	Bending Moment (j) (kip-in)	Axial force (kips)
1	132.8	-104.4	-15.92	31	8.6	-7.7	-12.95
2	104.4	-94.7	-16.37	32	7.7	-6.5	-12.97
3	94.7	-86.5	-17.06	33	6.5	-5.6	-13.02
4	88.5	-80.0	-16.73	34	5.6	-3.6	-13.08
5	80.0	-54.6	-17.22	35	3.6	-1.5	-13.15
6	54.6	-30.6	-17.78	38	1.5	2.9	-13.29
7	30.6	-3.7	-18.10	37	-2.9	9.1	-13.49
8	3.7	12.4	-18.17	38	-9.1	18.5	-13.78
9	-12.4	23.1	-18.14	39	-18.5	30.9	-14.23
10	-23.1	30.6	-18.03	40	-30.9	34.5	-14.61
11	-30.6	47.9	-17.67	41	-34.5	38.9	-14.82
12	-47.9	52.2	-17.02	42	-38.9	42.8	-15.06
13	-52.2	52.0	-16.48	43	-42.8	46.6	-15.33
14	-51.9	49.8	-16.03	44	-46.6	49.8	-15.65
15	-49.8	46.6	-15.65	45	-49.8	51.9	-16.03
16	-46.6	42.8	-15.33	46	-51.9	52.1	-16.48
17	-42.8	38.9	-15.06	47	-52.1	47.9	-17.02
18	-38.9	34.6	-14.82	48	-47.9	30.6	-17.67
19	-34.6	30.9	-14.61	49	-30.6	23.0	-18.03
20	-30.9	18.8	-14.23	50	-23.0	12.4	-18.14
21	-18.6	9.2	-13.78	51	-12.4	-3.7	-18.17
22	-9.2	2.8	-13.49	52	3.7	-30.7	-18.10
23	-2.8	-1.5	-13.29	53	30.7	-54.6	-17.78
24	1.5	-3.7	-13.15	54	54.6	-80.1	-17.22
25	3.7	-5.6	-13.06	55	80.1	-85.9	-17.40
28	5.6	-6.5	-13.02	56	85.9	-94.7	-16.50
27	6.5	-7.7	-12.97	57	94.7	-105.3	-16.39
28	7.7	-8.6	-12.95	58	105.3	-132.7	-15.92
29	8.6	-9.1	-12.93				
30	9.1	-8.6	-12.93				

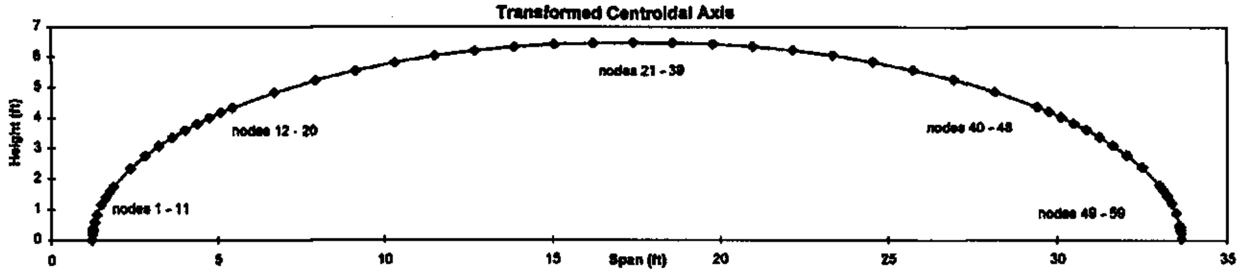

Table A-3. Displacements in Melan-Emperger Arch (dead load).

Node no.	x (in)	y (in)	Rotation (rad)	Node no.	x (in)	y (in)	Rotation (rad)
1	0.00e+00	0.00e+00	0.00e+00	31	-4.86e-06	-2.57e-04	2.19e-05
2	-4.67e-08	-2.90e-07	1.22e-06	32	-9.25e-06	-2.46e-04	4.20e-05
3	-8.98e-08	-4.08e-07	1.62e-06	33	-1.27e-05	-2.27e-04	5.96e-05
4	-1.40e-07	-5.03e-07	1.93e-06	34	-1.49e-05	-2.02e-04	7.30e-05
5	-1.81e-07	-5.79e-07	2.16e-06	35	-1.56e-05	-1.73e-04	8.22e-05
6	-4.21e-07	-9.03e-07	2.98e-06	36	-1.45e-05	-1.42e-04	8.68e-05
7	-7.88e-07	-1.25e-08	3.60e-06	37	-1.19e-05	-1.09e-04	8.57e-05
8	-1.41e-06	-1.68e-06	3.98e-08	38	-7.93e-06	-7.79e-05	7.79e-05
9	-1.94e-06	-1.98e-06	3.90e-06	39	-3.21e-06	-5.01e-05	6.39e-05
10	-2.39e-06	-2.23e-06	3.59e-06	40	1.42e-06	-2.77e-05	4.49e-05
11	-2.78e-06	-2.44e-06	3.13e-06	41	2.51e-06	-2.27e-05	3.90e-05
12	-4.15e-06	-3.43e-06	-7.10e-08	42	3.43e-06	-1.83e-05	3.30e-05
13	-4.89e-06	-4.67e-06	-4.46e-06	43	4.21e-06	-1.44e-05	2.69e-05
14	-5.18e-06	-6.32e-06	-9.52e-06	44	4.78e-06	-1.12e-05	2.09e-05
15	-5.12e-06	-8.49e-06	-1.51e-05	45	5.12e-06	-8.48e-06	1.51e-05
16	-4.78e-06	-1.12e-05	-2.09e-05	46	5.18e-06	-6.32e-06	9.51e-06
17	-4.20e-06	-1.45e-05	-2.69e-05	47	4.89e-06	-4.66e-06	4.45e-06
18	-3.42e-06	-1.83e-05	-3.30e-05	48	4.15e-06	-3.43e-06	6.59e-08
19	-2.50e-06	-2.27e-05	-3.91e-05	49	2.78e-06	-2.43e-06	-3.14e-06
20	-1.40e-08	-2.77e-05	-4.50e-05	50	2.39e-06	-2.22e-06	-3.59e-06
21	3.23e-06	-5.01e-05	-6.39e-05	51	1.94e-06	-1.98e-06	-3.90e-06
22	7.96e-06	-7.80e-05	-7.80e-05	52	1.41e-06	-1.68e-06	-3.98e-06
23	1.19e-05	-1.09e-04	-8.58e-05	53	7.87e-07	-1.24e-06	-3.60e-06
24	1.45e-05	-1.42e-04	-8.68e-05	54	4.21e-07	-9.01e-07	-2.98e-06
25	1.56e-05	-1.74e-04	-8.21e-05	55	1.81e-07	-5.79e-07	-2.16e-06
26	1.49e-05	-2.02e-04	-7.29e-05	56	1.34e-07	-5.02e-07	-1.93e-06
27	1.27e-05	-2.27e-04	-5.95e-05	57	8.98e-08	-4.06e-07	-1.62e-06
28	9.28e-06	-2.46e-04	-4.19e-05	58	4.67e-08	-2.90e-07	-1.22e-06
29	4.90e-06	-2.57e-04	-2.18e-05	59	0.00e+00	0.00e+00	0.00e+00
30	1.16e-08	-2.62e-04	6.14e-08				

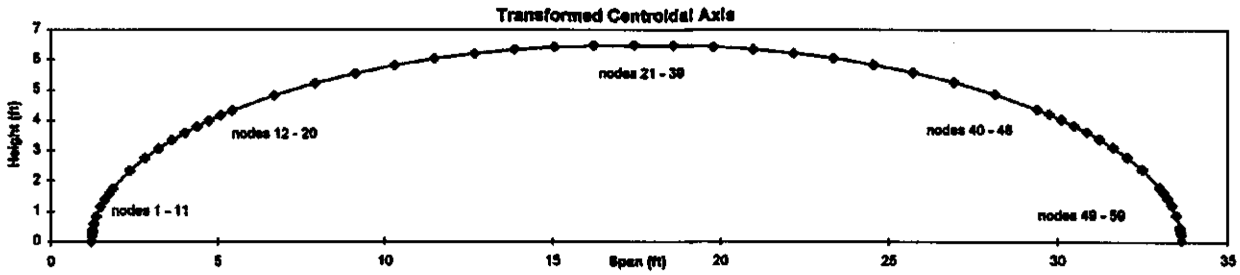

Table A-4. Concrete and Steel Stresses in Melan-Emperger Arch (dead load).

Node no.	Stress at Intrados (psi)	Stress at Extrados (psi)	Stress in Steel (psi)	Node no.	Stress at Intrados (psi)	Stress at Extrados (psi)	Stress in Steel (psi)
1	10.73	-40.87	45.21	31	-21.17	-60.51	-378.05
2	4.85	-35.92	4.25	32	-23.26	-57.21	-377.30
3	2.34	-34.80	-21.49	33	-25.89	-53.03	-374.10
4	1.09	-32.97	-30.39	34	-27.24	-49.09	-367.81
5	-0.54	-32.54	-43.61	35	-30.40	-43.14	-363.49
6	-6.08	-28.65	-87.76	36	-32.82	-37.54	-360.07
7	-11.48	-24.89	-130.78	37	-37.47	-29.36	-366.99
8	-18.05	-19.78	-182.63	38	-42.12	-20.83	-383.93
9	-22.62	-16.40	-218.12	39	-48.93	-11.85	-412.57
10	-26.12	-13.81	-244.66	40	-53.39	-2.77	-445.81
11	-30.36	-11.81	-280.09	41	-53.56	-1.25	-428.86
12	-40.43	-4.33	-350.94	42	-53.77	0.31	-433.62
13	-46.64	-0.30	-389.69	43	-53.10	1.10	-435.35
14	-50.80	2.00	-412.57	44	-51.83	1.38	-433.12
15	-53.70	3.25	-426.32	45	-49.72	0.92	-426.32
16	-55.51	3.51	-433.12	46	-46.48	-0.46	-412.57
17	-56.55	3.08	-435.35	47	-42.03	-2.73	-389.69
18	-56.85	2.04	-433.62	48	-35.64	-6.33	-350.94
19	-56.43	0.28	-428.66	49	-28.13	-11.81	-280.09
20	-58.68	-0.11	-445.81	50	-25.29	-13.73	-244.66
21	-53.19	-9.78	-412.57	51	-21.83	-16.00	-218.12
22	-46.14	-20.69	-383.93	52	-17.37	-19.00	-182.63
23	-39.66	-30.70	-366.99	53	-10.92	-23.62	-130.78
24	-34.16	-39.38	-360.07	54	-5.54	-27.37	-87.76
25	-31.03	-45.30	-363.49	55	-0.81	-32.38	-43.61
26	-27.63	-51.09	-367.61	56	1.15	-32.55	-30.39
27	-25.83	-54.63	-374.10	57	2.93	-34.04	-21.49
28	-23.29	-58.39	-377.30	58	5.39	-35.54	4.25
29	-21.12	-61.11	-378.05	59	10.73	-40.87	45.21
30	-19.97	-62.26	-377.15				

APPENDIX B: LUTEN ARCH

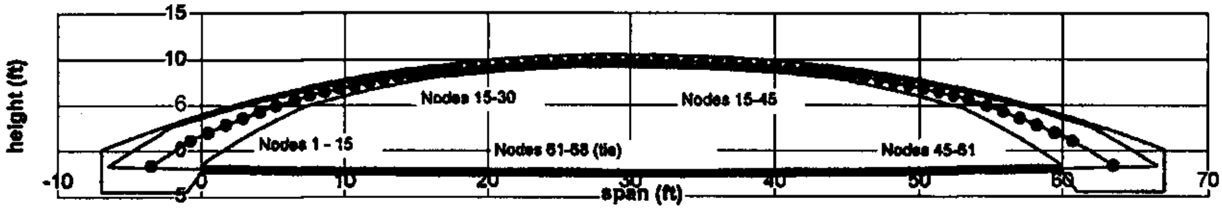

Table B-1. Displacements in Luten Arch without "lip" (dead load).

Node no.	x (in)	y (in)	Rotation (rad)	Node no.	x (in)	y (in)	Rotation (rad)
1	0.00e+00	0.00e+00	0.00e+00	36	-4.63e-03	-9.11e-02	3.52e-04
2	-5.81e-04	-5.86e-04	-1.50e-06	37	-5.02e-03	-8.64e-02	4.11e-04
3	-8.71e-04	-8.74e-04	-5.45e-06	38	-5.31e-03	-8.10e-02	4.63e-04
4	-1.15e-03	-1.22e-03	-1.02e-05	39	-5.50e-03	-7.51e-02	5.04e-04
5	-1.41e-03	-1.66e-03	-1.86e-05	40	-5.52e-03	-8.87e-02	5.34e-04
6	-1.64e-03	-2.21e-03	-2.87e-05	41	-5.32e-03	-6.21e-02	5.55e-04
7	-1.83e-03	-2.96e-03	-4.38e-05	42	-5.16e-03	-5.52e-02	5.65e-04
8	-1.96e-03	-4.21e-03	-7.78e-05	43	-4.87e-03	-4.83e-02	5.58e-04
9	-2.00e-03	-5.64e-03	-1.15e-04	44	-4.62e-03	-4.15e-02	5.31e-04
10	-1.92e-03	-7.53e-03	-1.53e-04	45	-4.25e-03	-3.53e-02	4.80e-04
11	-1.71e-03	-9.87e-03	-1.91e-04	46	-3.62e-03	-2.93e-02	4.18e-04
12	-1.42e-03	-1.27e-02	-2.30e-04	47	-3.05e-03	-2.43e-02	3.65e-04
13	-1.05e-03	-1.60e-02	-2.72e-04	48	-2.54e-03	-1.99e-02	3.17e-04
14	-6.11e-04	-1.98e-02	-3.15e-04	49	-2.10e-03	-1.61e-02	2.73e-04
15	-1.10e-04	-2.42e-02	-3.63e-04	50	-1.72e-03	-1.27e-02	2.32e-04
16	4.50e-04	-2.92e-02	-4.16e-04	51	-1.43e-03	-9.91e-03	1.92e-04
17	1.07e-03	-3.51e-02	-4.78e-04	52	-1.22e-03	-7.56e-03	1.54e-04
18	1.37e-03	-4.13e-02	-5.25e-04	53	-1.13e-03	-5.66e-03	1.16e-04
19	1.68e-03	-4.80e-02	-5.51e-04	54	-1.17e-03	-4.22e-03	7.83e-05
20	2.03e-03	-5.48e-02	-5.59e-04	55	-1.29e-03	-2.97e-03	4.41e-05
21	2.25e-03	-6.17e-02	-5.55e-04	56	-1.48e-03	-2.22e-03	2.70e-05
22	2.32e-03	-6.83e-02	-5.38e-04	57	-1.72e-03	-1.66e-03	1.68e-05
23	2.30e-03	-7.48e-02	-5.08e-04	58	-1.97e-03	-1.23e-03	1.03e-05
24	2.12e-03	-8.08e-02	-4.67e-04	59	-2.25e-03	-8.75e-04	5.51e-06
25	1.83e-03	-8.62e-02	-4.15e-04	60	-2.54e-03	-5.87e-04	1.54e-06
26	1.45e-03	-9.09e-02	-3.55e-04	61	-3.12e-03	0.00e+00	0.00e+00
27	9.74e-04	-9.48e-02	-2.90e-04	62	-4.15e-03	-2.71e-03	1.20e-04
28	4.29e-04	-9.79e-02	-2.22e-04	83	-5.51e-03	-7.43e-01	9.16e-03
29	-2.08e-04	-1.00e-01	-1.51e-04	64	9.10e-03	-1.74e+00	6.54e-03
30	-8.85e-04	-1.02e-01	-7.73e-05	65	-1.56e-03	-2.16e+00	-1.96e-09
31	-1.59e-03	-1.02e-01	-1.60e-06	86	-1.22e-02	-1.74e+00	-6.54e-03
32	-2.29e-03	-1.02e-01	7.41e-05	67	2.39e-03	-7.43e-01	-9.16e-03
33	-2.97e-03	-1.00e-01	1.48e-04	68	1.03e-03	-2.71e-03	-1.20e-04
34	-3.61e-03	-9.81e-02	2.19e-04				
35	-4.16e-03	-9.50e-02	2.86e-04				

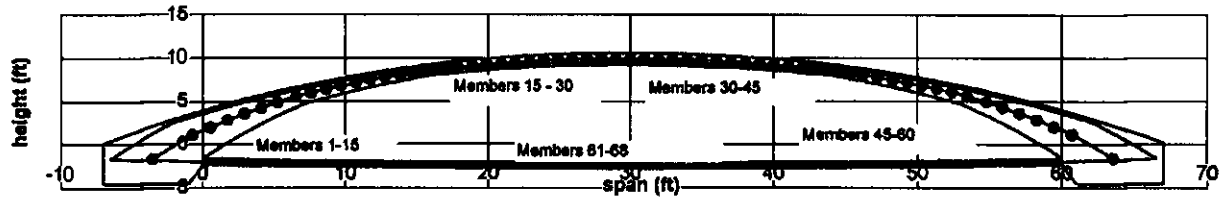

Table B-2. Member Forces in Luten Arch without "lip" (dead load).

Member no.	Bending moment (i) (lb-ft)	Bending moment (j) (lb-ft)	Axial force (lb)	Member no.	Bending moment (i) (lb-ft)	Bending moment (j) (lb-ft)	Axial force (lb)
1	3.45e+04	1.10e+05	-5.38e+05	35	6.92e+04	-6.46e+04	-4.12e+05
2	-1.10e+05	9.33e+04	-5.13e+05	36	6.46e+04	-5.75e+04	-4.12e+05
3	-9.33e+04	8.28e+04	-4.98e+05	37	5.75e+04	-4.77e+04	-4.13e+05
4	-8.28e+04	8.85e+04	-4.85e+05	38	4.77e+04	-3.53e+04	-4.13e+05
5	-8.85e+04	9.95e+04	-4.74e+05	39	3.53e+04	-2.41e+04	-4.14e+05
6	-9.95e+04	1.14e+05	-4.64e+05	40	2.41e+04	-1.88e+04	-4.15e+05
7	-1.14e+05	1.26e+05	-4.56e+05	41	1.88e+04	-1.46e+03	-4.16e+05
8	-1.26e+05	1.07e+05	-4.50e+05	42	1.46e+03	1.50e+04	-4.17e+05
9	-1.07e+05	9.24e+04	-4.45e+05	43	-1.50e+04	3.91e+04	-4.19e+05
10	-9.24e+04	8.38e+04	-4.40e+05	44	-3.92e+04	5.87e+04	-4.20e+05
11	-8.38e+04	7.45e+04	-4.36e+05	45	-5.87e+04	5.99e+04	-4.23e+05
12	-7.45e+04	6.79e+04	-4.33e+05	46	-5.99e+04	6.08e+04	-4.25e+05
13	-6.79e+04	6.34e+04	-4.30e+05	47	-6.08e+04	6.38e+04	-4.27e+05
14	-6.34e+04	6.04e+04	-4.27e+05	48	-6.38e+04	6.83e+04	-4.30e+05
15	-6.04e+04	5.96e+04	-4.25e+05	49	-6.83e+04	7.50e+04	-4.33e+05
16	-5.96e+04	5.75e+04	-4.23e+05	50	-7.50e+04	8.43e+04	-4.36e+05
17	-5.75e+04	3.47e+04	-4.20e+05	51	-8.43e+04	9.29e+04	-4.40e+05
18	-3.47e+04	1.48e+04	-4.19e+05	52	-9.28e+04	1.07e+05	-4.45e+05
19	-1.48e+04	2.38e+03	-4.18e+05	53	-1.07e+05	1.28e+05	-4.50e+05
20	-2.37e+03	-1.08e+04	-4.16e+05	54	-1.26e+05	1.15e+05	-4.56e+05
21	1.08e+04	-2.43e+04	-4.15e+05	55	-1.15e+05	1.00e+05	-4.64e+05
22	2.43e+04	-3.55e+04	-4.14e+05	56	-1.00e+05	8.92e+04	-4.74e+05
23	3.55e+04	-4.79e+04	-4.13e+05	57	-8.92e+04	8.35e+04	-4.85e+05
24	4.79e+04	-5.76e+04	-4.13e+05	58	-8.35e+04	9.41e+04	-4.98e+05
25	5.76e+04	-6.47e+04	-4.12e+05	59	-9.41e+04	1.11e+05	-5.13e+05
26	6.47e+04	-6.93e+04	-4.12e+05	60	-1.11e+05	-3.36e+04	-5.38e+05
27	6.93e+04	-7.11e+04	-4.11e+05	61	2.77e+05	-2.33e+05	4.14e+05
28	7.11e+04	-7.49e+04	-4.11e+05	62	2.33e+05	1.14e+03	4.11e+05
29	7.49e+04	-7.64e+04	-4.11e+05	63	-1.14e+03	6.62e+04	4.11e+05
30	7.64e+04	-7.96e+04	-4.11e+05	64	-6.62e+04	1.02e+05	4.11e+05
31	7.96e+04	-7.64e+04	-4.11e+05	65	-1.02e+05	6.62e+04	4.11e+05
32	7.64e+04	-7.49e+04	-4.11e+05	66	-6.62e+04	1.14e+03	4.11e+05
33	7.49e+04	-7.11e+04	-4.11e+05	67	-1.14e+03	-2.33e+05	4.11e+05
34	7.11e+04	-6.92e+04	-4.11e+05				

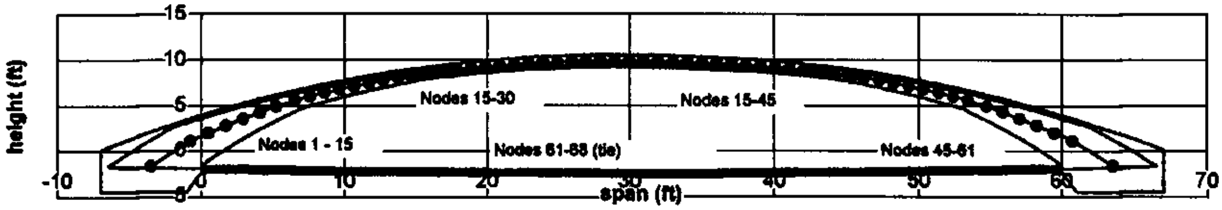

Table B-3. Concrete and Steel Stresses in Luten Arch without "lip" (dead load).

	Concrete stress (ksi)				Steel stress (ksi)		
Node no.	Stress due to axial force	Stress due to bending moment	Stress at intrados	Stress at extrados	Stress due to axial force	Stress due to bending moment	Total steel stress
1	-0.0528	0.0034	-0.0495	-0.0562	-0.5284	0.0316	-0.5600
2	-0.0661	-0.0191	-0.0853	-0.0470	-0.6613	-0.1693	-0.4920
3	-0.0723	-0.0207	-0.0930	-0.0516	-0.7232	-0.1792	-0.5440
4	-0.0798	-0.0236	-0.1034	-0.0562	-0.7982	-0.1995	-0.5987
5	-0.0890	-0.0329	-0.1219	-0.0561	-0.8896	-0.2695	-0.6201
6	-0.1002	-0.0489	-0.1491	-0.0513	-1.0021	-0.3858	-0.6183
7	-0.1159	-0.0777	-0.1935	-0.0382	-1.1585	-0.5898	-0.5688
8	-0.1290	-0.1105	-0.2395	-0.0184	-1.2897	-0.7362	-0.5535
9	-0.1342	-0.1039	-0.2382	-0.0303	-1.3424	-0.6739	-0.6685
10	-0.1398	-0.0998	-0.2396	-0.0400	-1.3983	-0.6286	-0.7697
11	-0.1457	-0.1003	-0.2460	-0.0454	-1.4570	-0.6125	-0.8445
12	-0.1519	-0.0987	-0.2506	-0.0532	-1.5189	-0.5826	-0.9363
13	-0.1584	-0.0993	-0.2577	-0.0590	-1.5838	-0.5659	-1.0179
14	-0.1651	-0.1023	-0.2674	-0.0628	-1.6513	-0.5617	-1.0896
15	-0.1721	-0.1073	-0.2794	-0.0648	-1.7213	-0.2802	-1.4411
16	-0.1791	-0.1160	-0.2951	-0.0631	-1.7913	-0.1935	-1.5978
17	-0.1814	-0.1162	-0.2976	-0.0651	-1.8136	-0.0934	-1.9070
18	-0.1799	-0.0896	-0.2495	-0.1103	-1.7990	-0.1105	-1.9095
19	-0.1790	-0.0294	-0.2085	-0.1496	-1.7905	-0.1023	-1.8928
20	-0.1782	-0.0047	-0.1829	-0.1735	-1.7817	-0.0225	-1.7593
21	-0.1774	0.0214	-0.1560	-0.1988	-1.7740	0.1021	-1.8760
22	-0.1767	0.0481	-0.1287	-0.2248	-1.7675	0.2296	-1.9970
23	-0.1761	0.0700	-0.1062	-0.2461	-1.7614	0.3346	-2.0960
24	-0.1757	0.0943	-0.0814	-0.2699	-1.7566	0.4514	-2.2080
25	-0.1753	0.1131	-0.0621	-0.2884	-1.7525	0.5424	-2.2949
26	-0.1749	0.1269	-0.0481	-0.3018	-1.7491	0.6087	-2.3578
27	-0.1746	0.1356	-0.0390	-0.3103	-1.7464	0.6513	-2.3977
28	-0.1744	0.1392	-0.0353	-0.3136	-1.7442	0.6687	-2.4129
29	-0.1743	0.1465	-0.0278	-0.3208	-1.7429	0.7043	-2.4472
30	-0.1742	0.1493	-0.0249	-0.3235	-1.7422	0.7179	-2.4601
31	-0.1742	0.1556	-0.0187	-0.3298	-1.7422	0.7482	-2.4904
32	-0.1742	-0.1492	-0.0250	-0.3234	-1.7422	-0.7176	-2.4598
33	-0.1743	-0.1464	-0.0279	-0.3207	-1.7429	-0.7039	-2.4468
34	-0.1744	-0.1390	-0.0354	-0.3135	-1.7442	-0.6681	-2.4123
35	-0.1746	-0.1354	-0.0392	-0.3101	-1.7464	-0.6504	-2.3968
36	-0.1749	-0.1266	-0.0483	-0.3015	-1.7491	-0.6076	-2.3567
37	-0.1753	-0.1129	-0.0624	-0.2881	-1.7525	-0.5410	-2.2935
38	-0.1757	-0.0939	-0.0817	-0.2696	-1.7566	-0.4498	-2.2064
39	-0.1761	-0.0696	-0.1065	-0.2457	-1.7614	-0.3328	-2.0942
40	-0.1767	-0.0477	-0.1291	-0.2244	-1.7675	-0.2275	-1.9950
41	-0.1775	-0.0372	-0.1403	-0.2147	-1.7748	-0.1302	-1.6448

	Concrete stress (ksi)				Steel stress (ksi)		
Node no.	Stress due to axial force	Stress due to bending moment	Stress at intrados	Stress at extrados	Stress due to axial force	Stress due to bending moment	Total steel stress
42	-0.1781	-0.0029	-0.1752	-0.1810	-1.7811	-0.0047	-1.7764
43	-0.1790	0.0300	-0.2090	-0.1490	-1.7899	0.0287	-1.8166
44	-0.1798	0.0785	-0.2583	-0.1014	-1.7981	0.1610	-1.6371
45	-0.1814	0.1188	-0.3002	-0.0626	-1.8144	0.4376	-1.3768
46	-0.1791	0.1166	-0.2957	-0.0625	-1.7913	0.5845	-1.2068
47	-0.1721	0.1079	-0.2800	-0.0642	-1.7213	0.5675	-1.1538
48	-0.1651	0.1029	-0.2680	-0.0623	-1.6514	0.5638	-1.0876
49	-0.1584	0.0999	-0.2583	-0.0585	-1.5838	0.5691	-1.0147
50	-0.1519	0.0992	-0.2511	-0.0527	-1.5190	0.5858	-0.9331
51	-0.1457	0.1009	-0.2466	-0.0448	-1.4570	0.6158	-0.8412
52	-0.1398	0.1003	-0.2401	-0.0395	-1.3983	0.6318	-0.7865
53	-0.1342	0.1044	-0.2387	-0.0298	-1.3424	0.6771	-0.6653
54	-0.1290	0.1110	-0.2400	-0.0180	-1.2897	0.7394	-0.5503
55	-0.1159	0.0781	-0.1939	-0.0378	-1.1586	0.5928	-0.5658
56	-0.1002	0.0492	-0.1494	-0.0510	-1.0022	0.3882	-0.6139
57	-0.0890	0.0331	-0.1221	-0.0558	-0.8896	0.2715	-0.6181
58	-0.0798	0.0238	-0.1036	-0.0560	-0.7983	0.2012	-0.5971
59	-0.0723	0.0208	-0.0932	-0.0515	-0.7232	0.1806	-0.5427
60	-0.0661	0.0193	-0.0854	-0.0469	-0.6613	0.1704	-0.4908
61	-0.0528	-0.0033	-0.0498	-0.0561	-0.5284	-0.0308	-0.5592
61	0.0916	0.1414	0.2329	-0.0498	0.9155	0.0000	0.9155
62	0.3298	1.8174	2.1471	-1.4876	3.2976	0.0000	3.2976
63	0.3297	-0.0089	0.3208	0.3386	3.2970	0.0000	3.2970
64	0.3294	-0.5159	-0.1865	0.8454	3.2944	0.0000	3.2944
65	0.3294	0.7916	-0.4622	1.1210	3.2944	0.0000	3.2944
66	0.3294	0.5159	-0.1865	0.8454	3.2944	0.0000	3.2944
67	0.3297	0.0089	0.3208	0.3386	3.2970	0.0000	3.2970
68	0.3298	-1.8174	2.1471	-1.4876	3.2976	0.0000	3.2976

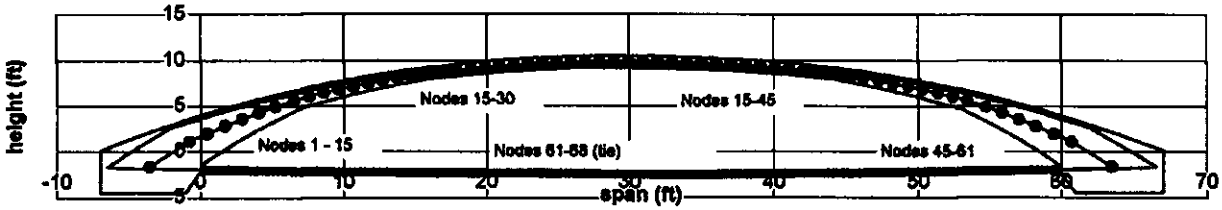

Table B-4. Displacements in Luten Arch with "lip" (dead load).

Node no.	x (in)	y (in)	Rotation (rad)	Node no.	x (in)	y (in)	Rotation (rad)
1	0.00e+00	0.00e+00	0.00e+00	35	1.86e-02	-1.81e-01	4.78e-04
2	-2.76e-04	-8.29e-04	-1.72e-05	36	1.84e-02	-1.74e-01	5.87e-04
3	-3.08e-04	-1.43e-03	-3.34e-05	37	1.83e-02	-1.66e-01	6.88e-04
4	-2.14e-04	-2.28e-03	-5.30e-05	38	1.84e-02	-1.57e-01	7.78e-04
5	3.28e-05	-3.44e-03	-7.77e-05	39	1.86e-02	-1.47e-01	8.53e-04
6	4.41e-04	-4.99e-03	-1.10e-04	40	1.91e-02	-1.37e-01	9.13e-04
7	1.06e-03	-7.09e-03	-1.56e-04	41	2.01e-02	-1.25e-01	9.59e-04
8	2.05e-03	-1.04e-02	-2.33e-04	42	2.09e-02	-1.13e-01	9.89e-04
9	2.95e-03	-1.40e-02	-3.13e-04	43	2.21e-02	-1.01e-01	9.95e-04
10	4.14e-03	-1.86e-02	-3.91e-04	44	2.32e-02	-8.92e-02	9.74e-04
11	5.58e-03	-2.42e-02	-4.70e-04	45	2.46e-02	-7.76e-02	9.22e-04
12	7.18e-03	-3.06e-02	-5.48e-04	46	2.67e-02	-6.60e-02	8.49e-04
13	8.94e-03	-3.81e-02	-6.25e-04	47	2.87e-02	-5.59e-02	7.77e-04
14	1.08e-02	-4.65e-02	-7.00e-04	48	3.07e-02	-4.66e-02	7.02e-04
15	1.28e-02	-5.58e-02	-7.75e-04	49	3.25e-02	-3.82e-02	6.26e-04
16	1.48e-02	-6.59e-02	-8.47e-04	50	3.43e-02	-3.07e-02	5.49e-04
17	1.68e-02	-7.75e-02	-9.21e-04	51	3.59e-02	-2.42e-02	4.71e-04
18	1.81e-02	-8.90e-02	-9.69e-04	52	3.74e-02	-1.87e-02	3.92e-04
19	1.94e-02	-1.01e-01	-9.88e-04	53	3.85e-02	-1.41e-02	3.13e-04
20	2.06e-02	-1.13e-01	-9.84e-04	54	3.94e-02	-1.04e-02	2.34e-04
21	2.16e-02	-1.25e-01	-9.59e-04	55	4.04e-02	-7.10e-03	1.57e-04
22	2.23e-02	-1.38e-01	-9.17e-04	58	4.11e-02	-5.00e-03	1.11e-04
23	2.28e-02	-1.47e-01	-8.57e-04	57	4.15e-02	-3.44e-03	7.78e-05
24	2.31e-02	-1.57e-01	-7.81e-04	58	4.17e-02	-2.28e-03	5.31e-05
25	2.32e-02	-1.66e-01	-6.91e-04	59	4.18e-02	-1.43e-03	3.35e-05
26	2.31e-02	-1.74e-01	-5.90e-04	80	4.18e-02	-8.30e-04	1.73e-05
27	2.28e-02	-1.80e-01	-4.81e-04	61	4.15e-02	0.00e+00	0.00e+00
28	2.25e-02	-1.86e-01	-3.67e-04	62	4.08e-02	-5.31e-03	2.34e-04
29	2.19e-02	-1.89e-01	-2.49e-04	63	3.41e-02	-6.36e-02	6.06e-04
30	2.14e-02	-1.92e-01	-1.26e-04	64	2.82e-02	-1.29e-01	4.22e-04
31	2.07e-02	-1.92e-01	-1.50e-06	65	2.08e-02	-1.56e-01	-7.67e-11
32	2.01e-02	-1.92e-01	1.23e-04	66	1.33e-02	-1.29e-01	-4.22e-04
33	1.95e-02	-1.89e-01	2.46e-04	67	7.44e-03	-6.36e-02	-6.06e-04
34	1.90e-02	-1.86e-01	3.64e-04	68	7.11e-04	-5.31e-03	-2.34e-04

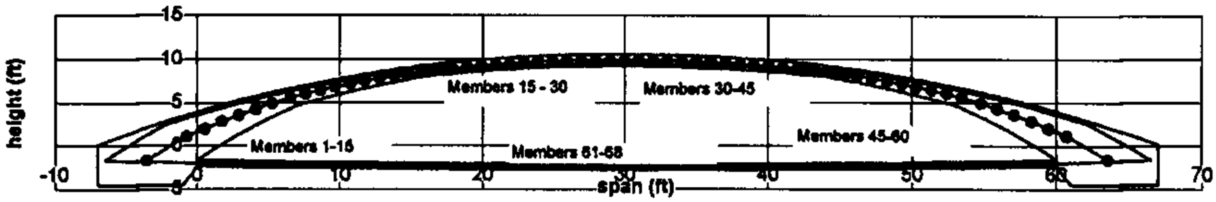

Table B-5. Member Forces in Luten Arch with "lip" (dead load).

Member no.	Bending moment (i) (lb-ft)	Bending moment (j) (lb-ft)	Axial force (lb)	Member no.	Bending moment (i) (lb-ft)	Bending moment (j) (lb-ft)	Axial force (lb)
1	-4.20e+05	4.44e+05	-5.07e+05	35	1.15e+05	-1.08e+05	-3.68e+05
2	-4.44e+05	3.89e+05	-4.77e+05	36	1.08e+05	-9.79e+04	-3.68e+05
3	-3.89e+05	3.42e+05	-4.61e+05	37	9.79e+04	-8.47e+04	-3.69e+05
4	-3.42e+05	3.15e+05	-4.47e+05	38	8.47e+04	-6.83e+04	-3.89e+05
5	-3.15e+05	2.95e+05	-4.36e+05	39	6.83e+04	-5.22e+04	-3.70e+05
6	-2.95e+05	2.81e+05	-4.26e+05	40	5.23e+04	-4.07e+04	-3.72e+05
7	-2.81e+05	2.63e+05	-4.17e+05	41	4.08e+04	-1.77e+04	-3.72e+05
8	-2.63e+05	2.26e+05	-4.09e+05	42	1.77e+04	5.40e+03	-3.74e+05
9	-2.26e+05	1.94e+05	-4.04e+05	43	-5.39e+03	3.61e+04	-3.75e+05
10	-1.94e+05	1.68e+05	-3.99e+05	44	-3.61e+04	6.36e+04	-3.77e+05
11	-1.68e+05	1.44e+05	-3.95e+05	45	-8.36e+04	7.62e+04	-3.80e+05
12	-1.44e+05	1.23e+05	-3.91e+05	48	-7.62e+04	8.90e+04	-3.82e+05
13	-1.23e+05	1.04e+05	-3.88e+05	47	-8.90e+04	1.05e+05	-3.85e+05
14	-1.04e+05	8.87e+04	-3.85e+05	48	-1.05e+05	1.23e+05	-3.88e+05
15	-8.87e+04	7.59e+04	-3.82e+05	49	-1.23e+05	1.44e+05	-3.91e+05
16	-7.59e+04	6.24e+04	-3.80e+05	50	-1.44e+05	1.69e+05	-3.95e+05
17	-6.24e+04	3.22e+04	-3.77e+05	51	-1.69e+05	1.94e+05	-3.99e+05
18	-3.22e+04	5.13e+03	-3.75e+05	52	-1.94e+05	2.26e+05	-4.04e+05
19	-5.13e+03	-1.43e+04	-3.74e+05	53	-2.26e+05	2.64e+05	-4.09e+05
20	1.43e+04	-3.36e+04	-3.73e+05	54	-2.64e+05	2.81e+05	-4.17e+05
21	3.36e+04	-5.24e+04	-3.71e+05	55	-2.81e+05	2.95e+05	-4.26e+05
22	5.24e+04	-6.85e+04	-3.70e+05	56	-2.95e+05	3.15e+05	-4.36e+05
23	6.84e+04	-8.48e+04	-3.69e+05	57	-3.15e+05	3.43e+05	-4.47e+05
24	8.48e+04	-9.81e+04	-3.69e+05	58	-3.43e+05	3.89e+05	-4.61e+05
25	9.81e+04	-1.08e+05	-3.66e+05	59	-3.89e+05	4.45e+05	-4.77e+05
26	1.08e+05	-1.15e+05	-3.68e+05	60	-4.45e+05	4.21e+05	-5.07e+05
27	1.15e+05	-1.20e+05	-3.67e+05	61	5.89e+05	-4.08e+05	3.72e+05
28	1.20e+05	-1.25e+05	-3.67e+05	62	4.08e+05	7.89e+03	3.67e+05
29	1.25e+05	-1.27e+05	-3.67e+05	83	-7.89e+03	1.90e+05	3.67e+05
30	1.27e+05	-1.30e+05	-3.66e+05	64	-1.90e+05	2.63e+05	3.66e+05
31	1.30e+05	-1.27e+05	-3.66e+05	65	-2.63e+05	1.90e+05	3.66e+05
32	1.27e+05	-1.25e+05	-3.67e+05	86	-1.90e+05	7.89e+03	3.67e+05
33	1.25e+05	-1.19e+05	-3.67e+05	87	-7.89e+03	-4.08e+05	3.67e+05
34	1.19e+05	-1.15e+05	-3.67e+05				

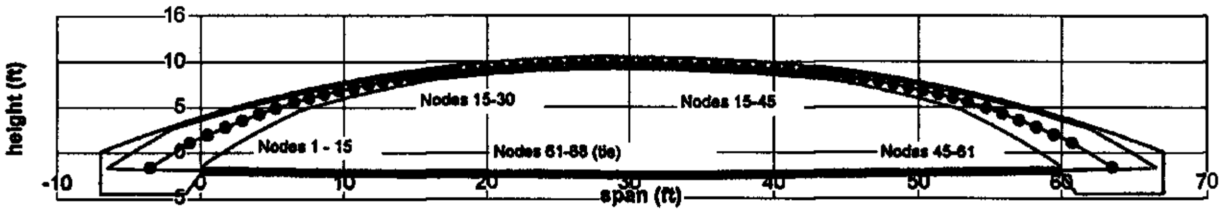

Table B-6. Concrete and Steel Stresses in Luten Arch with "lip" (dead load).

	Concrete stress (ksi)				Steel stress (ksi)		
Node no.	Stress due to axial force	Stress due to bending moment	Stress at intrados	Stress at extrados	Stress due to axial force	Stress due to bending moment	Total steel stress
1	-0.04975	-0.04046	-0.09020	-0.0092940	-0.49749	-0.38448	-0.113010
2	-0.06151	-0.07617	-0.13768	0.0146519	-0.61514	-0.68400	0.068865
3	-0.06699	-0.08478	-0.15175	0.0177790	-0.66986	-0.74594	0.076082
4	-0.07370	-0.09599	-0.16970	0.0222901	-0.73704	-0.82456	0.087522
5	-0.08185	-0.11478	-0.19864	0.0329283	-0.81854	-0.95733	0.138790
6	-0.09192	-0.14211	-0.23403	0.0501933	-0.91918	-1.14255	0.223368
7	-0.10588	-0.18732	-0.29320	0.0814400	-1.05879	-1.45030	0.391504
8	-0.11725	-0.22680	-0.34405	0.1095495	-1.17249	-1.54121	0.368723
9	-0.12182	-0.21558	-0.33740	0.0937583	-1.21823	-1.42588	0.207645
10	-0.12670	-0.20521	-0.33191	0.0785128	-1.26701	-1.31832	0.051310
11	-0.13177	-0.19768	-0.32945	0.0659120	-1.31769	-1.23069	-0.087000
12	-0.13717	-0.18667	-0.32385	0.0494997	-1.37173	-1.12354	-0.248190
13	-0.14284	-0.17598	-0.31882	0.0331443	-1.42837	-1.02137	-0.407000
14	-0.14874	-0.16576	-0.31450	0.0170258	-1.48739	-0.92515	-0.562230
15	-0.15487	-0.15506	-0.30993	0.0001972	-1.54867	-0.41115	-1.137520
16	-0.16097	-0.14562	-0.30659	-0.0153460	-1.60970	-0.24665	-1.363040
17	-0.16261	-0.12433	-0.28694	-0.0382890	-1.62614	-0.10138	-1.727530
18	-0.16120	-0.06354	-0.22474	-0.0976570	-1.61198	-0.10236	-1.714330
19	-0.18039	-0.01010	-0.17049	-0.1502820	-1.60386	-0.03561	-1.639470
20	-0.15949	0.02796	-0.13153	-0.1874460	-1.59489	0.13527	-1.730160
21	-0.15870	0.06559	-0.09311	-0.2242830	-1.58697	0.31792	-1.904890
22	-0.15805	0.10194	-0.05611	-0.2599930	-1.58052	0.49497	-2.075490
23	-0.15743	0.13273	-0.02470	-0.2901600	-1.57431	0.64542	-2.219740
24	-0.15696	0.16416	0.00720	-0.3211160	-1.56956	0.79932	-2.368880
25	-0.15655	0.18938	0.03283	-0.3459340	-1.56552	0.92319	-2.488710
26	-0.15821	0.20870	0.05249	-0.3649150	-1.56214	1.01838	-2.580500
27	-0.15594	0.22231	0.06637	-0.3782550	-1.55944	1.08566	-2.645100
28	-0.15572	0.22996	0.07423	-0.3856780	-1.55723	1.12372	-2.680940
29	-0.15559	0.23964	0.08405	-0.3952280	-1.55591	1.17160	-2.727510
30	-0.15552	0.24403	0.08852	-0.3995510	-1.55517	1.19348	-2.748650
31	-0.15552	0.25023	0.09471	-0.4057500	-1.55518	1.22399	-2.779170
32	-0.15552	-0.24400	0.08848	-0.3995160	-1.55518	-1.19330	-2.748480
33	-0.15559	-0.23956	0.08397	-0.3951500	-1.55591	-1.17121	-2.727130
34	-0.15572	-0.22982	0.07410	-0.3855460	-1.55723	-1.12307	-2.680300
35	-0.15594	-0.22213	0.06618	-0.3780720	-1.55945	-1.08476	-2.644210
36	-0.15621	-0.20849	0.05228	-0.3647050	-1.56214	-1.01734	-2.579480
37	-0.15655	-0.18911	0.03256	-0.3456640	-1.56553	-0.92187	-2.487400
38	-0.15696	-0.18387	0.00691	-0.3208250	-1.56957	-0.79790	-2.367470
39	-0.15743	-0.13240	-0.02504	-0.2898300	-1.57433	-0.64381	-2.218140
40	-0.15805	-0.10157	-0.05648	-0.2596240	-1.58054	-0.49317	-2.073710
41	-0.15882	-0.07966	-0.07917	-0.2384820	-1.58824	-0.28259	-1.305650

	Concrete stress (ksi)				Steel stress (ksi)		
Node no.	Stress due to axial force	Stress due to bending moment	Stress at intrados	Stress at extrados	Stress due to axial force	Stress due to bending moment	Total steel stress
42	-0.15940	-0.03474	-0.12466	-0.1941450	-1.59403	-0.05708	-1.536950
43	-0.16030	0.01062	-0.17092	-0.1496800	-1.60300	0.00957	-1.612580
44	-0.18108	0.07117	-0.23225	-0.0899080	-1.81081	0.14848	-1.462330
45	-0.16271	0.12596	-0.28867	-0.0367580	-1.82713	0.47400	-1.153130
46	-0.16098	0.14551	-0.30649	-0.0154760	-1.60982	0.74399	-0.865830
47	-0.15487	0.15530	-0.31016	0.0004258	-1.54869	0.83117	-0.717530
48	-0.14874	0.16598	-0.31472	0.0172348	-1.48742	0.92638	-0.561040
49	-0.14284	0.17851	-0.31935	0.0336750	-1.42839	1.02448	-0.403930
50	-0.13718	0.18720	-0.32438	0.0500270	-1.37178	1.12673	-0.245030
51	-0.13177	0.19820	-0.32997	0.0664293	-1.31770	1.23392	-0.083790
52	-0.12670	0.20572	-0.33243	0.0790184	-1.26704	1.32159	0.054547
53	-0.12183	0.21607	-0.33790	0.0942452	-1.21826	1.42911	0.210857
54	-0.11725	0.22727	-0.34452	0.1100223	-1.17250	1.54443	0.371932
55	-0.10588	0.18772	-0.29360	0.0818345	-1.05880	1.45338	0.394556
56	-0.09192	0.14242	-0.23434	0.0504966	-0.91920	1.14500	0.225803
57	-0.08185	0.11504	-0.19689	0.0331808	-0.81855	0.95944	0.140894
58	-0.07371	0.09620	-0.16991	0.0224923	-0.73707	0.82632	0.089256
59	-0.06699	0.08493	-0.15192	0.0179463	-0.86988	0.74742	0.077553
60	-0.06151	0.07630	-0.13782	0.0147904	-0.61513	0.88524	0.070109
61	-0.04975	0.04054	-0.09029	-0.0092110	-0.49749	0.10190	-0.395590
	Concrete tie stress (ksi)				Steel tie stress (ksi)		
	Stress due to axial force	Stress due to bending moment	Stress at top	Stress at bottom	Stress due to axial force	Stress due to bending moment	Total steel stress
	0.08237	0.23482	-0.15245	0.3171971			
	0.19142	0.22784	-0.03643	0.4192610	1.91418	0.03478	1.948957
	0.19139	-0.00440	0.19579	0.1869856	1.91388	0.83851	2.752389
	0.19107	-0.10614	0.29721	0.0849322	1.91073	1.16024	3.070973
	0.19107	-0.14687	0.33794	0.0442065	1.91073	0.83851	2.749240
	0.19107	-0.10614	0.29721	0.0849322	1.91073	0.03478	1.945506
	0.19139	-0.00440	0.19579	0.1869855	1.91388	-1.79996	0.113917
	0.19142	0.16295	0.02847	0.3543687	1.91418	-1.85511	0.059069

APPENDIX C: MARSH ARCH

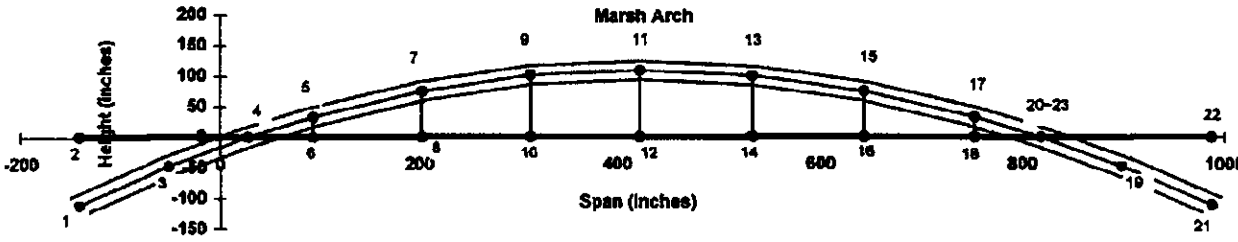

Table C-1. Displacements in Marsh Arch.

Deed Loed				Live Load			
Node no.	x (in)	y (in)	Rotation (rad)	Node no.	x (in)	y (in)	Rotation (rad)
1	0.00e+00	0.00e+00	0.00e+00	1	0.00e+00	0.00e+00	0.00e+00
2	3.18e-02	0.00e+00	0.00e+00	2	4.38e-02	0.00e+00	0.00e+00
3	8.62e-03	-3.02e-02	-5.35e-04	3	1.25e-02	-3.96e-02	-7.09e-04
4	3.18e-02	-8.60e-02	-6.52e-04	4	4.38e-02	-1.13e-01	-8.53e-04
5	4.27e-02	-1.23e-01	-3.75e-04	5	5.86e-02	-1.80e-01	-4.94e-04
6	3.19e-02	-1.23e-01	-4.37e-04	6	4.38e-02	-1.13e-01	-8.53e-04
7	4.23e-02	-1.54e-01	-1.23e-04	7	5.86e-02	-1.98e-01	-1.28e-04
8	3.24e-02	-1.57e-01	-1.67e-04	8	4.44e-02	-2.03e-01	-1.84e-04
9	3.29e-02	-1.59e-01	5.42e-05	9	4.58e-02	-1.98e-01	1.57e-04
10	2.17e-02	-1.63e-01	3.33e-05	10	4.49e-02	-2.03e-01	1.30e-04
11	3.35e-02	-1.45e-01	2.01e-04	11	3.19e-02	-1.68e-01	3.53e-04
12	3.24e-02	-1.49e-01	1.98e-04	12	4.54e-02	-1.73e-01	3.51e-04
13	3.29e-02	-1.59e-01	5.42e-05	13	2.41e-02	-1.20e-01	4.39e-04
14	3.19e-02	-1.63e-01	3.33e-05	14	4.57e-02	-1.25e-01	4.54e-04
15	4.23e-02	-1.54e-01	-1.23e-04	15	2.45e-02	-6.67e-02	4.42e-04
16	3.18e-02	-1.57e-01	-1.67e-04	16	4.58e-02	-6.95e-02	4.93e-04
17	4.27e-02	-1.23e-01	-3.75e-04	17	3.22e-02	-1.28e-02	4.28e-04
18	3.18e-02	-1.23e-01	-4.37e-04	18	4.58e-02	-1.45e-02	4.01e-04
19	8.62e-03	-3.02e-02	-5.35e-04	19	2.50e-02	1.40e-02	-2.51e-04
20	3.18e-02	-8.60e-02	-6.52e-04	20	3.60e-02	1.26e-02	1.85e-04
21	0.00e+00	0.00e+00	0.00e+00	21	0.00e+00	0.00e+00	0.00e+00
22	3.45e-02	0.00e+00	0.00e+00	22	4.58e-02	0.00e+00	0.00e+00

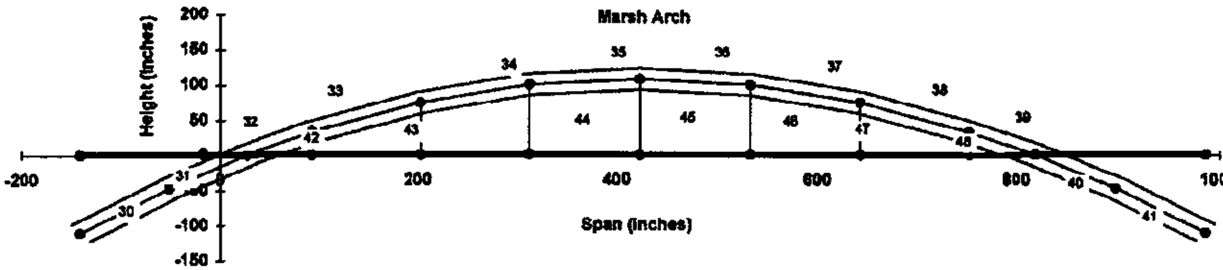

Table C-2. Concrete Member Forces in Marsh Arch.

Deed Loed				Live Load			
Member no.	Bending moment (i) (kip-in)	Bending moment (j) (kip-in)	Axial force (kips)	Member no.	Bending moment (i) (kip-in)	Bending moment (j) (kip-in)	Axial force (kips)
1	-7.11e+02	6.74e+02	-1.82e+02	1	-9.57e+02	8.78e+02	-2.22e+02
2	-6.74e+02	-3.15e+02	-1.79e+02	2	-8.78e+02	-4.36e+02	-2.18e+02
3	-4.40e+02	-8.84e+02	-1.73e+02	3	6.53e+02	-7.46e+02	-2.07e+02
4	2.62e+02	-1.84e+02	-1.75e+02	4	4.95e+02	-3.89e+02	-2.18e+02
5	2.43e+02	-1.34e+02	-1.70e+02	5	4.66e+02	-2.49e+02	-2.07e+02
6	2.41e+02	-7.75e+01	-1.69e+02	6	4.49e+02	-5.55e+01	-1.98e+02
7	7.75e+01	-2.41e+02	-1.69e+02	7	3.23e+02	1.02e+02	-1.94e+02
8	1.34e+02	-2.43e+02	-1.70e+02	8	1.87e+02	1.81e+02	-1.93e+02
9	1.84e+02	-2.62e+02	-1.75e+02	9	1.10e+02	1.42e+02	-1.92e+02
10	8.84e+02	4.40e+02	-1.73e+02	10	-1.43e+02	8.06e+02	-2.06e+02
11	3.15e+02	6.74e+02	-1.79e+02	11	-8.06e+02	5.32e+02	-2.08e+02
12	-6.74e+02	7.11e+02	-1.82e+02	12	-5.32e+02	-1.18e+03	-2.10e+02
13	1.62e+02	2.15e+02	7.70e+00	13	1.67e+02	2.35e+02	1.11e+01
14	5.31e+00	2.19e+01	1.71e+01	14	-5.12e+01	-2.98e+01	2.28e+01
15	-3.88e+01	-3.29e+01	1.76e+01	15	-1.33e+02	-1.26e+02	2.31e+01
16	-7.12e+01	-7.05e+01	1.74e+01	16	-1.78e+02	-1.77e+02	2.08e+01
17	-3.88e+01	-3.29e+01	1.76e+01	17	-1.92e+02	-1.97e+02	1.88e+01
18	5.31e+00	2.19e+01	1.71e+01	18	-1.94e+02	-2.13e+02	1.57e+01
19	1.62e+02	2.15e+02	7.70e+00	19	8.15e-01	2.45e+01	2.21e+01
20	-1.16e+03	-2.99e+02	0.00e+00	20	-1.51e+03	-3.93e+02	0.00e+00
21	9.17e+01	-6.36e+02	5.35e+00	21	1.45e+02	-8.08e+02	5.70e+00
22	2.68e+02	-2.76e+02	2.52e+01	22	4.06e+02	-3.76e+02	2.68e+01
23	2.39e+02	-1.64e+02	2.58e+01	23	4.27e+02	-2.05e+02	2.50e+01
24	2.21e+02	-1.11e+02	2.46e+01	24	4.21e+02	-2.36e+01	2.05e+01
25	2.31e+02	-5.43e+01	2.23e+01	25	3.28e+02	1.22e+02	1.48e+01
26	2.52e+02	4.00e+01	1.84e+01	26	2.15e+02	1.36e+02	8.09e+00
27	2.71e+02	2.88e+02	1.03e+01	27	2.29e+02	4.15e+02	-1.33e+00
28	-8.77e+02	1.40e+03	0.00e+00	28	-4.57e+02	9.04e+02	0.00e+00
29	0.00e+00	0.00e+00	0.00e+00	29	0.00e+00	0.00e+00	0.00e+00

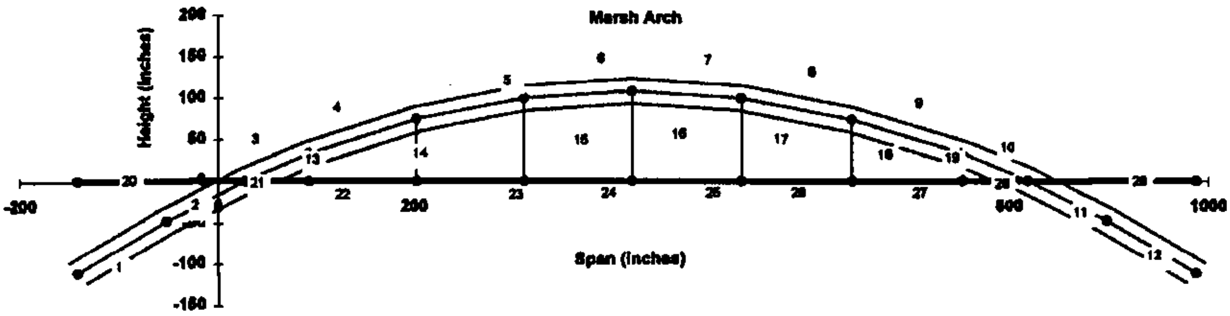

Table C-3. Steel Member Forces in Marsh Arch.

Dead Load				Live Load			
Member no.	Bending moment (i) (kip-in)	Bending moment (j) (kip-in)	Axial force (kips)	Member no.	Bending moment (i) (kip-in)	Bending moment (j) (kip-in)	Axial force (kips)
1	-1.00e+02	9.50e+01	-2.17e+01	1	-1.35e+02	1.24e+02	-2.64e+01
2	-9.50e+01	-4.44e+01	-2.13e+01	2	-1.24e+02	-6.15e+01	-2.60e+01
3	7.01e+01	-8.19e+01	-2.04e+01	3	9.21e+01	-1.05e+02	-2.47e+01
4	4.77e+01	-3.80e+01	-2.17e+01	4	6.98e+01	-5.49e+01	-2.59e+01
5	3.69e+01	-2.60e+01	-2.09e+01	5	6.58e+01	-3.51e+01	-2.46e+01
6	3.42e+01	-1.89e+01	-2.03e+01	6	6.33e+01	-7.83e+00	-2.36e+01
7	3.40e+01	-1.09e+01	-2.01e+01	7	4.55e+01	1.43e+01	-2.31e+01
8	3.44e+01	3.73e+00	-2.01e+01	8	2.64e+01	2.56e+01	-2.29e+01
9	3.19e+01	3.81e+01	-2.02e+01	9	1.55e+01	2.00e+01	-2.28e+01
10	-2.14e+01	9.28e+01	-2.01e+01	10	-2.01e+01	1.14e+02	-2.45e+01
11	-9.28e+01	6.20e+01	-2.04e+01	11	-1.14e+02	7.50e+01	-2.47e+01
12	-6.20e+01	-1.25e+02	-2.06e+01	12	-7.50e+01	-1.66e+02	-2.50e+01
13	1.15e+02	1.53e+02	2.20e+00	13	1.19e+02	1.67e+02	3.18e+00
14	3.79e+00	1.56e+01	4.90e+00	14	-3.65e+01	-2.13e+01	6.51e+00
15	-2.77e+01	-2.35e+01	5.03e+00	15	-9.50e+01	-8.96e+01	6.59e+00
16	-5.07e+01	-5.03e+01	4.98e+00	16	-1.27e+02	-1.27e+02	5.93e+00
17	-7.92e+01	-8.24e+01	4.87e+00	17	-1.37e+02	-1.40e+02	5.30e+00
18	-1.20e+02	-1.29e+02	4.52e+00	18	-1.38e+02	-1.52e+02	4.47e+00
19	-5.62e+01	-8.34e+01	3.19e+00	19	5.83e+01	1.74e+01	6.30e+00

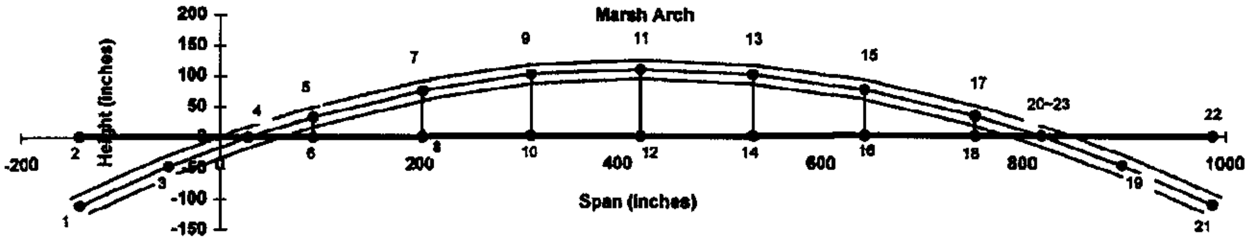

Table C-4. Concrete and Steel Stresses in Marsh Arch.

Dead Load						Live Load					
Node no.	Axiel stress	Bending moment stress	Stress et intredos	Stress at extredos	Stress in steel	Node no.	Axiel stress	Bending moment stress	Stress at intredos	Stress et extrados	Stress in steel
Arch						Arch					
1	-0.269	-0.226	-0.515	-0.063	-0.0385	1	-0.352	-0.304	-0.655	-0.048	-0.0469
3	-0.264	-0.214	-0.496	-0.070	-0.0379	3	-0.346	-0.279	-0.625	-0.086	-0.0462
4	-0.272	0.158	-0.114	-0.430	-0.0363	4	-0.329	0.207	-0.122	-0.538	-0.0439
5	-0.269	0.107	-0.162	-0.396	-0.0385	5	-0.345	0.157	-0.168	-0.502	-0.0460
7	-0.278	0.083	-0.195	-0.361	-0.0371	7	-0.326	0.146	-0.160	-0.478	-0.0438
9	-0.270	0.077	-0.193	-0.347	-0.0361	9	-0.315	0.142	-0.173	-0.457	-0.0420
11	-0.267	0.076	-0.191	-0.344	-0.0357	11	-0.306	0.102	-0.205	-0.410	-0.0410
13	-0.266	-0.025	-0.244	-0.293	-0.0358	13	-0.308	0.032	-0.338	-0.273	-0.0408
15	-0.269	0.008	-0.278	-0.261	-0.0359	15	-0.304	0.056	-0.382	-0.247	-0.0406
17	-0.268	0.066	-0.354	-0.182	-0.0357	17	-0.328	0.045	-0.371	-0.261	-0.0435
20	-0.271	0.209	-0.480	-0.062	-0.0362	20	-0.330	0.256	-0.586	-0.074	-0.0440
19	-275.000	0.140	-0.414	-0.135	-0.0366	19	-0.333	0.169	-0.502	-0.164	-0.0444
21	-0.329	-0.261	-0.049	-0.610	-0.0439	21	-0.329	-0.375	0.045	-0.704	-0.0439
Verticals						Verticals					
5	0.055	0.035	0.020	0.090	0.0138	5	0.079	0.036	0.044	0.115	0.0199
8	0.055	0.046	0.101	0.009	0.0138	6	0.079	0.050	0.130	0.029	0.0199
7	0.122	0.001	0.121	0.124	0.0308	7	0.163	-0.011	0.174	0.152	0.0407
6	0.122	0.005	0.127	0.116	0.0306	8	0.163	-0.006	0.156	0.189	0.0407
9	0.126	-0.008	0.134	0.118	0.0315	9	0.185	-0.029	0.193	0.138	0.0412
10	0.126	-0.007	0.119	0.133	0.0315	10	0.165	-0.027	0.136	0.192	0.0412
11	0.125	-0.015	0.140	0.109	0.0312	11	0.148	-0.038	0.168	0.110	0.0371
12	0.125	-0.015	0.110	0.140	0.0312	12	0.148	-0.038	0.110	0.186	0.0371
13	0.122	-0.024	0.148	0.098	0.0305	13	0.133	-0.041	0.174	0.091	0.0331
14	0.122	-0.025	0.097	0.147	0.0305	14	0.133	-0.042	0.090	0.175	0.0331
15	0.113	-0.036	0.149	0.077	0.0263	15	0.112	-0.042	0.153	0.070	0.0260
16	0.113	-0.039	0.074	0.152	0.0283	16	0.112	-0.046	0.066	0.156	0.0280
17	0.060	-0.017	0.097	0.063	0.0200	17	0.158	0.000	0.157	0.156	0.0394
18	0.080	-0.025	0.055	0.105	0.0200	16	0.158	0.005	0.163	0.152	0.0394
Deck	Axial stress	Bending moment stress	Stress at top	Stress et bottom		Deck	Axiel stress	Bending moment stress	Stress et top	Stress at bottom	
2	0.000	-0.251	-0.251	0.251		2	0.000	-0.328	-0.328	0.326	
4	0.003	0.020	0.023	-0.017		4	0.003	0.031	0.035	-0.028	
8	0.015	0.058	0.073	-0.044		6	0.016	0.066	0.104	-0.073	
6	0.015	0.052	0.067	-0.037		8	0.014	0.093	0.107	-0.078	
10	0.014	0.046	0.062	-0.034		10	0.012	0.091	0.103	-0.079	
12	0.013	0.050	0.063	-0.037		12	0.009	0.071	0.060	-0.083	
14	0.011	-0.012	0.022	-0.001		14	0.005	0.026	-0.022	0.031	
16	0.006	0.009	-0.003	0.015		16	-0.001	0.030	-0.030	0.029	
16	0.000	0.063	-0.063	0.063		16	0.000	0.090	-0.900	0.090	
20	0.000	0.303	-0.303	0.303		20	0.000	0.196	-0.196	0.196	
22	0.000	0.000	0.000	0.000		22	0.000	0.000	0.000	0.000	